



Review article

Liquid organic hydrogen carriers for transportation and storing of renewable energy – Review and discussion

Päivi T. Aakko-Saksa^{a,b,*}, Chris Cook^c, Jari Kiviaho^b, Timo Repo^a^a University of Helsinki, P.O. Box 55, FI-00014, University of Helsinki, Helsinki, Finland^b VTT Technical Research Centre of Finland Ltd., P.O.Box 1000, FI-02044, VTT, Espoo, Finland^c University of York, York, UK

HIGHLIGHTS

- Solutions are needed for storing and transporting the renewable energy.
- Hydrogen storage options are reviewed and discussed.
- Some end-use sectors are more demanding than the others.
- Liquid organic hydrogen carriers are promising hydrogen storages.
- The “circular” methanol and hydrocarbons or are also promising hydrogen storages.

ARTICLE INFO

Keywords:

Hydrogen

Liquid organic hydrogen carriers

Energy storage

Dibenzyl toluene

Methanol

ABSTRACT

Transition to renewable energy systems is essential to achieve the climate change mitigation targets. However, the timing and the regions of the production and consumption of the renewable energy do not always match, and different energy storage technologies are needed to secure the uninterrupted energy supply. Liquid organic hydrogen carriers (LOHCs) offer a flexible media for the storage and transportation of renewable energy. These “liquid hydrogen batteries” are reversibly hydrogenated and dehydrogenated using catalysts at elevated temperatures. Commercial LOHC concepts are already available. Another flexible route to store energy is through “circular” hydrogen carriers, such as methanol and methane produced from atmospheric carbon dioxide (CO₂). These fuels have a long history as fossil fuels. In this review, the chemistry and state-of-the-art of LOHCs are explored and discussed against defined criteria with comparison made to existing energy storage systems. The LOHCs and “circular” hydrogen carriers were found to be particularly promising hydrogen storage systems.

1. Introduction

Fossil energy reserves are sufficient for hundreds of years at the current rate of energy consumption. However, the threat of climate change may end the era of fossil energy before the reserves are depleted. In 2013, world total primary energy supply (TPES) was 13 555 Mtoe (570 EJ), 13.5% of this was produced by renewable energy sources; mainly by traditional biomass used for heating and cooking in developing countries (73.4%) and hydroelectric power (17.8%) [1]. The “New Policies Scenario” of the International Energy Agency (IEA) [2] projected that the share of renewables in the primary energy will be 18% by 2035 as the hydropower, bioenergy, wind and solar photovoltaic (PV) increases. Renewable energy is estimated to cover from 100 EJ to 400 EJ of world energy production by 2050 [3]. In 2013, for

the first time more capacity was added for renewable power than for coal, natural gas, and oil combined [4].

The need for novel energy storage media arises from the imbalances between regions for production and consumption of renewable energy and the fluxionality of its generation. For example, the regions best suited for the production of renewable energy are often far away from the greatest demand. Consequently, long-distance and overseas transport of energy is needed. In the northern latitudes, the potential for solar energy production is at the highest over the summer season, when the energy consumption is at the lowest. Wind conditions may change rapidly. Overall, the irregular production of renewable energy is challenging. Even hydropower capacity is not fully utilized over the low consumption periods.

Feasible energy storages are needed to remove the bottlenecks of

* Corresponding author. University of Helsinki, Laboratory of Inorganic Chemistry, A.I.Virtasen aukio 1, P.O. Box 55, FI-00014, University of Helsinki, Finland.
E-mail address: paivi.aakko-saksa@helsinki.fi (P.T. Aakko-Saksa).

the deployment of the renewable energy in large scale in order to improve energy security and balance the energy prices. Oil, gas and coal are excellent energy storages, while the other energy storage technologies have their pros and cons; there are differences in the size classes, on the duration of the storage periods and on the energy transport capabilities. For example, duration of discharge is short for compressed air and pumped hydro energy storages. Batteries are available from kW to over 100 MW, but their gravimetric energy density is low and electricity cannot be stored in batteries for extensive time periods. One type of energy storage does not fit in all purposes. For example, aviation and long-distance ground transport are dependent on the high-quality liquid fuels, while the power and heat sector, as well as shipping, can cope with more challenging fuels.

Hydrogen creates possibilities for transportation and long-term storage of renewable energy. Recently, the IEA [5] defined hydrogen as a flexible energy carrier, which can be produced from any energy source, and which can be converted into various energy forms. The main challenges with hydrogen implementation are related to its production and storage. In energy equivalents, global annual hydrogen demand (172 Mtoe, 60 Mt) is below 2% of the world energy production. Approximately 48% of hydrogen is produced from natural gas (NG) using steam methane reforming (SMR), 30% is a by-product from the petroleum refining, 18% is produced from coal, and 4% from water electrolysis [5]. In the US, 59% of hydrogen is produced on-purpose in oil refineries and ammonia plants, and almost 36% as a by-product from catalytic reforming at oil refineries and at chlor-alkali plants [6]. In future, biomass or organic wastes could be hydrogen sources via the gasification, and carbon-neutral hydrogen could be produced by water electrolysis using electricity based on renewables or nuclear power. Ball and Wietschel et al. [3] found direct use of solar and wind to be the most efficient forms to produce hydrogen when the yield per hectare was evaluated; more efficient than producing electricity from biomass. Prices of hydrogen produced from NG vary regionally (\$0.9 per kg in the US, \$2.2 per kg in Europe and \$3.2 per kg in Japan) [5]. Price of hydrogen produced by distributed wind is \$7–11 per kg, by solar \$10–30 per kg and by electrolysis \$6–7 per kg when delivered with grid power in the US. Hydrogen produced by gasification from biomass was estimated as from \$1.50 to \$3.50 per kg at large-scale [6]. Lipman [6] estimated that the future cost of hydrogen produced by wind and solar have the potential price of \$3–4 per kg.

Use of hydrogen as an energy carrier demands effective, safe, user-friendly and economical storage. In general, hydrogen can be compressed (CH₂), liquefied (LH₂) or binded into solid or liquid storage materials for later use in turbines, in internal combustion engines (ICEs), in high-efficiency fuel cells (FCs) or for chemicals (Fig. 1). Hydrogen can be stored in an underground cavern or in a pressurised tank until it is re-electrified. Hydrogen can also be physically adsorbed in metals and high surface area adsorbents. By forming a chemical bond, hydrogen can be stored in hydrides, boranes and liquid organic hydrogen carriers (LOHCs). Low temperatures or high pressures are essential to store hydrogen by physisorption, while elevated temperatures

are needed to release hydrogen stored by chemisorption. Solid systems require a new infrastructure, while liquids can use the existing fuel infrastructure. Reversible hydrogen carriers can be hydrogenated and dehydrogenated without need to produce a new batch of material for every cycle (Fig. 2). Hydrogen can also be converted irreversibly into synthetic liquid fuels, such as methanol, methane, liquid hydrocarbons, formic acid, ammonia and its derivatives. These “circular” hydrogen carriers cannot be regenerated meaning that new batch of material is needed for each cycle (Fig. 3) as is the case with traditional fossil fuels. However, when circular hydrogen carriers are produced from renewable hydrogen and atmospheric CO₂ or nitrogen, the total cycle is carbon-neutral in contrary to fossil fuels [7–9].

LOHCs are regarded as newcomers in the energy storage field, though the concept was initially suggested already in the 1970's. Hydrogenation of aromatics and dehydrogenation of cyclic hydrocarbons are mature industrial processes, for example in oil refineries. Using the LOHC concept on a smaller scale requires new processes and catalysts with priority placed on the selectivity, safety, robustness and fast kinetics of the system, even at the cost of increased expenses. Organic species other than cyclic hydrocarbons warrant investigation as LOHCs if the thermodynamics of both hydrogenation and hydrogen release are favourable. In this work, chemical status of the LOHC concept is reviewed. Hydrogen storage in LOHC is discussed against the defined criteria and compared with compressed and liquid hydrogen as well as with solid and circular hydrogen carriers.

2. Liquid organic hydrogen carriers

2.1. Principle

LOHCs are liquids or low-melting solids that can be reversibly hydrogenated and dehydrogenated at elevated temperatures in the presence of catalyst. The initial structure of the LOHC compounds remain the same after the rechargeable hydrogen is released, while traditional fossil fuels and circular CO₂-based fuels are combusted as a whole. As the core structure of the LOHC remains untouched, production of new carrier in every cycle is avoided [9]. Clear benefits of LOHCs are their compatibility with the existing fuel infrastructure, and their capability to store hydrogen without losses even in the long-term or when transported overseas under standard conditions. The purity of the hydrogen released from LOHCs is high. Catalyst design aims at high selectivity at sufficiently mild reaction conditions to avoid breaking of the covalent carbon-carbon bond (or bonds with heteroatoms), and consequent cracking and coking [7,10]. Some chemical structures are more susceptible for hydrogenation or dehydrogenation than the others. Some common rules for the design of the compounds with favourable thermodynamics have been identified:

- Heterocyclic compounds, particularly bicyclic heteroarenes, are favourable due to decreased aromaticity of the molecule [7,9,11,12].
- A 5-membered heterocyclic ring is favourable [7].
- NH or NR in the 1-position of a hydrocarbon ring is favourable. The N–H bond is weaker than the C–H bond, and the C–H bonds adjacent to an N atom are weaker than the C–H bonds adjacent to C atom [7]. Steric hindrance around N-atom increases the dehydrogenation rate [13].
- N atoms or substituents in an 1,3-arrangement are favourable, but certain azoles, e.g., imidazole, are resistant towards hydrogenation [7].
- Favourable hydrogen binding enthalpies of LOHCs are sufficient to secure stability of the hydrogenated molecule and to achieve acceptable dehydrogenation temperature. Wild et al. [14] defined the desired enthalpy range from 40 to 70 kJ mol^{−1} H₂ and Cooper et al. [15] from 42 to 54 kJ mol^{−1} H₂.
- Increasing the number of fused aromatic rings decreases the hydrogenation enthalpies, however, the large polyaromatic

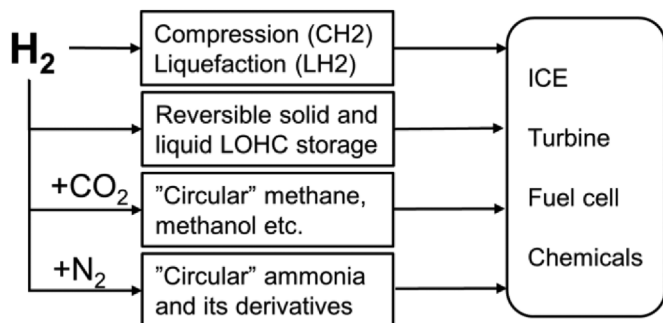


Fig. 1. Utilisation of the renewable energy through hydrogen storage pathways.

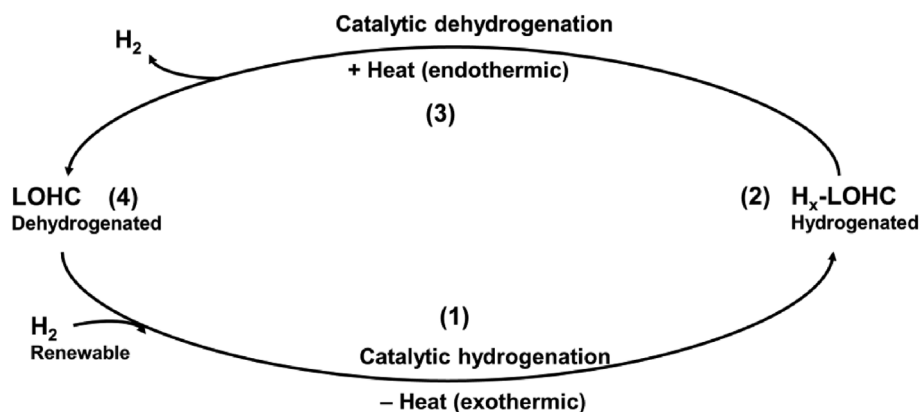


Fig. 2. Schematic illustration of the LOHC concept: (1) LOHC liquid is hydrogenated (2) hydrogenated LOHC liquid is transported to end-user (3) hydrogen is released (4) “empty” LOHC liquid (dehydrogenated form) is transported to the hydrogenation site.

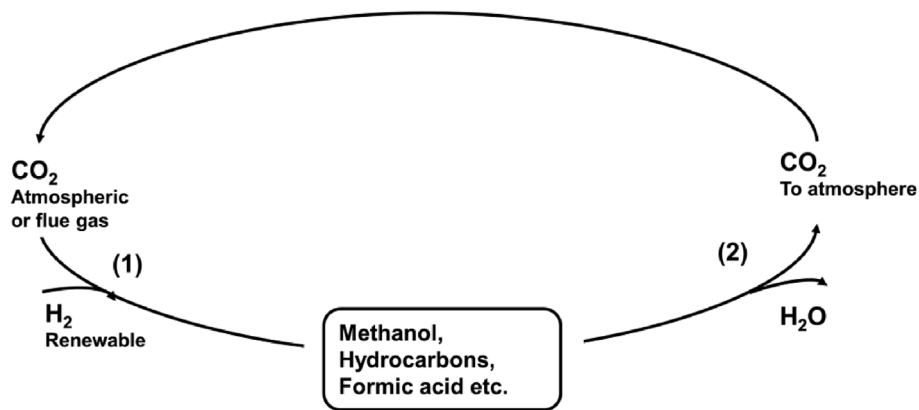


Fig. 3. Schematic illustration of the circular hydrogen carrier cycle. (1) Hydrogen and CO₂ is converted to “circular” hydrogen carriers, e.g. methanol or hydrocarbons (2) these are used in ICEs, FCs, turbines or as a feedstock for e.g. chemicals. Finally CO₂ is released in atmosphere (re-use in step 1).

compounds are solids [15].

- Dehydrogenation is more favourable for alkyl-substituted cyclic hydrocarbons [16] and for the five-membered rings than for the six-membered rings [15].

Examples of the dehydrogenation temperatures of some molecules without use of catalyst are shown in Supporting material. For example, dehydrogenation temperature for benzene is 300–350 °C (one aromatic ring), for naphthalene 250–300 °C (two fused aromatic rings) and for N-containing heteroaromatics 50–200 °C (from one to three rings) [15].

Heterogeneous metal catalysts assist hydrogenation and dehydrogenation in the LOHC systems [17]. For example, hydrogenation of LOHCs with Ru or Ni catalysts takes place at temperatures of 100–250 °C and pressures of 10–50 bar. Hydrogenation of LOHCs is exothermic, and thus excess heat can be recovered, or cooling is needed. Endothermic dehydrogenation is typically catalysed by heterogeneous Pt or Pd catalysts at temperatures of 150–400 °C and pressures below 10 bar. Support is also important for the activity and stability of a heterogeneous catalyst. Homogenous catalysts typically operate at lower temperatures than heterogeneous catalysts [7]. However, they often require a solvent, and their durability may be modest.

In the following Sections, only cyclic hydrocarbons and N-heterocyclic LOHC candidates are presented, though heterocyclic compounds possessing O, P and B (such as azaboranes) have also been studied [18,19], as well as some alicyclic and nonheterocyclic N-containing compounds [20].

2.2. Cyclic hydrocarbons

2.2.1. General

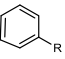
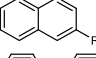
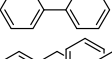
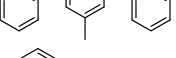
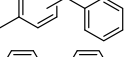
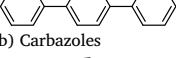
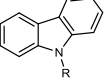
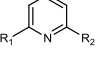
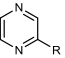
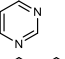
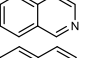
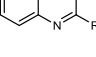
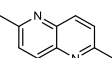
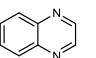
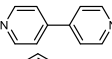
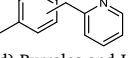
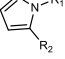
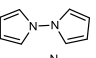
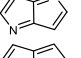
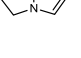
Many cyclic hydrocarbons could be used as LOHCs, for example benzene/cyclohexane (**a1**), toluene/methylcyclohexane (**a2**), naphthalene/decalin (**a3**) and biphenyl/bicyclohexyl (**a5**) (Table 1). Many of these compounds are widely used as industrial chemicals, for example the global volume of benzene and toluene is approximately 50 Mt annually at a price below 1 € per kg [18,21,22]. However, some of the aromatic compounds are carcinogenic or flammable (e.g. **a1** and **a2**) and some are solids at normal temperatures (e.g. **a3**, **a4**, **a5**). Hydrogen storage capacities of the cyclic hydrocarbons are in a range of 6–8 wt%, and the heat of hydrogenation and dehydrogenation is reasonable being in the range of 62–71 kJ mol^{−1} H₂ [18,23,24].

The hydrogenation of the aromatic compounds is commercial process, while the respective dehydrogenation processes are not as common because aromatics can be extracted easily from crude oil. At temperatures over 400 °C with a fix-bed reactor, catalysts have been observed to suffer from coke deposition resulting in the catalyst deactivation [23]. The development of stable dehydrogenation catalysts with sufficient activity is necessary for decentralized use.

Recently, dibenzyl and benzyl toluenes (DBT **a6**, BT **a7**) were introduced commercially as LOHCs by German company Hydrogenious GmbH (<http://www.hydrogenious.net>) [21]. The toluene LOHC system (**a2**) has been studied for many uses [25,26]. In Japan, Chiyoda Corporation (www.chiyodacorp.com) has demonstrated the use of the toluene LOHC system, called SPERA.

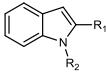
Table 1

Examples of cyclic compounds and their theoretical hydrogen storage capacities.

Hydrogen deficient form	Compound or Substituent	Hydrogen deficient mp(°C)/bp (°C)	Hydrogenated form mp(°C)/bp (°C)	Enthalpy difference ΔH (kJ mol ⁻¹ H ₂)	H ₂ storage capacity wt%
a) Hydrocarbons					
	(a1) Benzene (R = -)	5.5/80 ^g	7/81 ^g	68.6 ^{d,e}	7.2
	(a2) R = Methyl	-95/111 ^g	-127/101 ^g	68.3 ^d	6.2
	(a3) Naphthalene (R = -)	80/218 ^g	-43/196(cis) -30/187 (trans) ^g	66.4 ^f 63.9 ^d	7.3
	(a4) R = Methyl	-22/245 ^g	-21/194 ^b	65.3 ^e	6.6
	(a5) Biphenyl	70 ^a /255 ^a	4 ^a /228 ^a		7.1
	(a6) Dibenzyl toluenes (DBT)	-39(-34) ^{c,e} /390 ^{c,e}	< -50 ^o , -58 ^k /371 ^o	62 ^e 65 ^k 71 ^c	6.2 [*]
	(a7) Benzyl toluenes (BT)	-30 ^f /280 ^c	-/-270 ^c	63.5 ^k 71 ^c	6.2
	(a8) Terphenyl (o-, m-, p-)	58,86,212/337,379,389 ^k			
b) Carbazoles					
	(b1) Carbazole (R = -)	245 ^a /355 ^a	58 ^b /264 ^b	51.1 ^f	6.7
	(b2) R = Methyl	90 ^b /309 ^b	53 ^b /264 ^b	-	6.3
	(b3) R = Ethyl (NEC)	69 ^a /378 ^a	H12: 84 ^b /281 ^b H8: 43 ^a /H4: 9 ^b /323 ^b	50.6 ^f 51.0 ⁱ 53 ^m	5.8
	(b4) R = Propyl (NPC)	48 ⁱ /336 ^b	-		5.5
	(b5) R = Butyl (NBC)	58 ^a /348 ^b	-		5.1
	(b6) R = Phenyl	95 ^a /415 ^a	-		6.6
	(b7) R = Acetyl	69 ^g /-	-		6.3
c) Pyridines and quinolines					
	(c1) Pyridine (R = -)	-42 ^a /115 ^a	-11 ^a /106 ^a	56.7 ^f 65.6 ^e	7.1
	(c2) R ₁ = Methyl	-70 ^a /129 ^a	-4 ^a /118 ^a		6.1
	(c3) R ₁ = Ethyl	-63 ^a /149 ^a	-5 ^b /143 ^a		5.3
	(c4) R ₁ = Propyl	2 ^a /170 ^a	-2 ^a /199 ^a liq./128 ^a		4.8
	(c7) R ₁ , R ₂ = Methyl	-6 ^a /145 ^a			5.3
	(c5) Pyrazine (R = -)	54 ^a /115 ^a	106 ^a /147 ^a		7.0
	(c6) R = Methyl	-29 ^a /135 ^a	62 ^a /156 ^a		6.0
	(c8) Pyrimidine	21 ^a /124 ^a	7 ^b /164 ^b		7.0
	(c9) Isoquinoline	25 ^a /243 ^a	27 ^b /212 ^b		7.2
	(c10) Quinoline (R = -)	-15 ^a /237 ^a	-40(cis) ^g , 48,75 ^{a,g} /200-205 ^g	61.9 ^e	7.2
	(c11) R = 2-Me	-2 ^a /248 ^a	35 ^b /225 ^b		6.6
	(c12) R = 3-Me				
	(c13) R = 8-Me				
	(c14) Dimethyl-1,5-naphthyridine				6.0
	(c15) Quinoxaline	29-32 ^a /220 ^a	55 ^b /242 ^b		7.2
	(c16) 4,4-Bipyridine	109-112 ^a /305 ^a	170-172 ^a /-		7.2
	(c17) 2-(N-methylbenzyl)pyridine (MBP)	-50(-46) ^a /-19(-18) ⁿ	291-293 ^a		6.2
d) Pyrroles and Indoles					
	(d1) Pyrrole (R = -)	-23 ^a /130 ^a	-63 ^a /87 ^a		5.6
	(d2) R ₁ = Methyl	-57 ^a /113 ^a	-90 ^a /81 ^a		4.7
	(d3) R ₁ = Ethyl	-41 ^b /129 ^a	-37 ^b /115 ^b		4.1
	(d4) R ₁ = Propyl	-28 ^b /145 ^a	-25 ^b /138 ^b		3.6
	(d5) R ₁ = Butyl (BuP)	-16 ^b /170 ^a	-13 ^b /154 ^a		3.2
	(d6) R ₁ = H, R ₂ = Methyl	-36 ^a /148 ^a	-28 ^a /99 ^b		4.7
	(d7) R ₁ = H, R ₂ = Ethyl	-14 ^b /164 ^a	-15 ^b /142 ^b		4.1
	(d8) R ₁ = H, R ₂ = Propyl	-3 ^b /191 ^b	-3 ^b /163 ^b		3.6
	(d9) R ₁ , R ₂ = Methyl	-34 ^b /130 ^b	-41 ^b /96 ^a		4.1
	(d10) 1,1-Bipyrrole	34 ^b /223 ^b	29 ^a /198 ^a		5.7
	(d11) Pyrrolopyrrole	17 ^b /180 ^b	33 ^b /201 ^b		7.1
	(d12) 1H-Pyrrolizene	-17 ^b /180 ^b	-15 ^b /142 ^b		5.6

(continued on next page)

Table 1 (continued)

Hydrogen deficient form	Compound or Substituent	Hydrogen deficient mp(°C)/bp (°C)	Hydrogenated form mp(°C)/bp (°C)	Enthalpy difference ΔH (kJ mol ⁻¹ H ₂)	H ₂ storage capacity wt%
	(d13) 1H-Indole (R = –)	53 ^a /254 ^a	86 ^a /186 ^a	51.9 (1xH ₂)	6.4
	(d14) R ₁ = H, R ₂ = Methyl (NMI)	30 ^a /239 ^a	4 ^b /181 ^b		5.7
	(d15) R ₁ = H, R ₂ = Ethyl (NEI)	–18 ⁱ , 40 ^b /253 ^a	15 ^b /20 ^b		5.2
	(d16) R ₁ = Methyl, R ₂ = H	60 ^a /273 ^a	25 ^b /205 ^b		5.7
	(d17) R ₁ R ₂ = Methyl	58 ^a /253 ^b	12 ^b /196 ^b		5.2
	(d18) Indolizine (IZ)	75 ^a 9 ^b /205 ^a	–4 ^b /166 ^b		6.4

* 1.9 kWh kg⁻¹ [21].

^a Experimental properties, Sigma Aldrich, Chem Spider.

^b Predicted, Chem Spider (US EPA EPI Suite).

^c Heat of desorption [24].

^d Heat of desorption [18].

^e Reaction enthalpy [21].

^f Reaction enthalpy, calculated [18].

^g CRC Handbook of Chemistry and Physics, 66th Edition.

^h [67].

ⁱ [66].

^j [101].

^k [45,58].

^l [23].

^m [60,61].

ⁿ [86].

^o [46].

2.2.2. Hydrogenation of aromatic hydrocarbons

The hydrogenation of aromatic hydrocarbons involves high pressures and temperatures [18]. The heat released in the exothermic hydrogenation is usually a favourable feature for the total energy balance of system, although cooling may be needed in stand-alone processes. Polynuclear arenes are hydrogenated more easily than benzene, especially at the outer rings where resonance-stabilization is lower. However, the alkyl substituents on the benzene ring inhibit hydrogenation. Naphthalenes are difficult to hydrogenate [11].

Heterogenous catalyst are used for the hydrogenation of aromatic hydrocarbons, for example, Rh, Ru, Co, Ni, Pd, Pt, Cr, W, Mo, Mn, Nb, and Ta based catalysts. Of these, noble metal catalysts are particularly effective. Benzene is hydrogenated to cyclohexane on an industrial scale using a Raney–Ni catalyst [11]. Benzene and monosubstituted alkyl benzenes have been hydrogenated using a commercial Ni catalyst at 95–125 °C and 20–40 atm [27]. Toluene has been hydrogenated at 50–100 °C and 10–50 bar [21]. Naphthalene and toluene have been hydrogenated using Ni and Pd–Ni catalysts supported on Si–Al [28]. An increased resistance to coking was observed in the toluene hydrogenation with higher loadings of Ni and incorporation of Pd in a mixed catalyst. Mild hydrogenation conditions have been achieved by using a slurry system consisting of metal alloys (LaNi₅, Mg₂Ni, and Raney–Ni) [18].

Naphthalene (a3) and 1,2,3,4-tetrahydronaphthalene (tetralin) have been hydrogenated in the liquid-phase in decane using a Ni catalyst at 80–160 °C and 20–40 bar [29]. Kirumakki et al. [30] hydrogenated a3 over NiO/SiO₂–Al₂O₃ catalysts with NiO on Al₂O₃ giving the best conversion (90%).

Sakanishi et al. [31] found that the catalysts activity towards the hydrogenation of anthracene and fluorene at a hydrogen pressure of 70 bars and at 100–250 °C increased in order of Rh > Pd > Pt > Ru. The carbon and alumina supports behaved similarly in the hydrogenation of polyaromatic hydrocarbons.

Nano-sized particles enhance the hydrogenation reactions. Sun et al. [32] found nanoRu@hectorite as an efficient and reusable catalyst for

the hydrogenation of benzene.

Homogenous hydrogenation of aromatic hydrocarbons is not as common as heterogenous hydrogenation due to lower catalyst efficiency and stability. The most effective homogenous catalysts for the hydrogenation of aromatic hydrocarbons are complexes containing Ru, Rh or Ir. Several homogeneous Ru catalysts hydrogenate benzene and its derivatives at 90 °C and 60 bar by using solvents in biphasic or aqueous systems with turn over frequencies (TOFs) from 20 to 2000. [Rh(5-C₅Me₅)Cl₂]₂ can hydrogenate benzene to cyclohexane at 50 °C and 50 bar in the presence of a base, which acts as a promoter and ties up HCl [11].

The French Institute of Petroleum (IFP) has patented a Ziegler-type homogenous catalyst for hydrogenation of aromatic hydrocarbons. Catalysts consist of at least two metal salts e.g., Ni and Co alkoxides, acetylacetonates or carboxylates, and a metal (e.g. Fe, Zn or Mo) with trialkylaluminum as a reducing agent. The arenes are hydrogenated at 155–180 °C and 10–30 bar in a solvent or in neat substrate. For example, 99% conversion of benzene was achieved with a substrate/metal ratio of 1829 [11].

Tethered complexes on supported metals (TCSM) are combined homogenous and heterogenous catalysts. RhCl(PPh₃)₂ moieties cross-linked to phosphinated styrene/divinylbenzene resin have shown activity in the hydrogenation of pyrene, tetralin, p-cresol, and methyl-naphthalene. Phenol has been hydrogenated to cyclohexanol with a TOF of 3400 using a Rh(N-N)/Pd-SiO₂ catalyst, whereas both Pd-SiO₂ and unsupported Rh(N-N) are inactive. Hydrogenation has also been conducted by using the cationic catalysts, such as [Rh(diphos)(cod)](SO₃CF₃), on Si containing supported Pd particles. Surface organometallics is one class capable for arene hydrogenation. Si- or Al-supported Ta, Ti, Zr and Hf hydrides can reduce benzene and alkyl-substituted benzenes with TOFs as high as 1000 [11].

The single-site supported organozirconium catalyst Cp*ZrBz₂/ZrS (Cp* = Me₅C₅, Bz = benzyl, ZrS = sulfated zirconia) catalyzes the hydrogenation of arene derivatives to the corresponding cyclohexanes. For example, xylenes were hydrogenated at 25 °C and 7 atm in 1 h [33].

Some metal-free systems have been discovered to be capable of hydrogen activation and consequently hydrogenation of substrates. Frustrated Lewis pairs (FLPs) consisting of Lewis acids and Lewis bases cannot interact directly due to steric hindrance, but they can activate molecular hydrogen and deliver the resulting proton (H^+) and hydride (H^-) to substrates. A variety of bases have proved to go through FLP hydrogenation [34]. Chernichenko et al. [35] reduced alkynes to alkanes by using FLP under mild conditions at 80 °C and 2 bar.

2.2.3. Dehydrogenation of cycloalkanes

The catalysts used for the dehydrogenation of cycloalkanes are most often based on Pt, or lower-cost Ni and Mo. Coking can be alleviated by adding a second metal, for example W, Ir, Re, Rh, Pd and/or a promoter, for example Ca, and by selecting a suitable support, for examples carbon nanofiber (CNF) or Al_2O_3 . Dehydrogenation of cyclic hydrocarbons typically requires relatively high temperature and carbonaceous deposit may be formed over the catalyst [18,36] through cleavage of the C–C bond of the aromatic ring on the acid sites of catalyst surface [23].

Catalytic reforming of cycloalkanes to aromatics is a well-known process in the refining industry, however, reforming is associated with isomerisation and cyclisation reactions besides dehydrogenation. The typical reforming catalysts are based on Pt and/or Re or other precious metals on alumina. Catalysts are poisoned by As, Cu, Pb and activity is reduced by S and N compounds that can be present in the crude oil based refinery streams. The reaction conditions range from temperatures of about 495–525 °C and pressures of about 5–45 atm [37]. Due to different targets of reforming and dehydrogenation of LOHCs, similar catalysts are not optimal for these processes, by default. Worth of noticing is also the absence of impurities in the LOHC chemicals.

Dehydrogenation of decalin to **a3** is easier than dehydrogenation of methylcyclohexane (MCH) to **a2**, and dehydrogenation of MCH is easier than dehydrogenation of cyclohexane to **a1**. Dehydrogenation of MCH progresses from 200 to 320 °C (99%), though conventional dehydrogenation catalysts requires temperatures over 400 °C [23]. Crabtree [7] reported of dehydrogenation of cyclohexane to **a1** over a Pt/alumite catalyst at 375 °C, and of high temperature needed also with the Pt–Rh catalyst. MCH has been dehydrogenated at 350 °C and at 3 bar [21]. Kariya et al. [38] dehydrogenated cyclohexane, MCH and decalin over Pt on activated carbon (AC) catalyst under “wet-dry multiphase conditions”. The highest initial rate of dehydrogenation was obtained for cyclohexane over Pt/AC at 350 °C. The addition of e.g. Mo, W, Re, Rh, Ir, Pd and Sn enhanced the dehydrogenation rate. A mixture of Pt/AC and Pd/AC catalysts showed higher activities than the Pt/AC alone. Standard formation enthalpy in dehydrogenation was +205.9 kJ mol⁻¹ for cyclohexane (68.6 kJ mol⁻¹ H₂), +204.8 kJ mol⁻¹ for MCH and 309.5 kJ mol⁻¹ and 332.5 kJ mol⁻¹ (61.9 and 66.5 kJ mol⁻¹ H₂) for decalin (cis, trans).

Hodoshima et al. [39] dehydrogenated decalin achieving conversions of almost 100% within 1 h at 280 °C with a Pt–Rh composite catalyst supported on granular AC in “superheated liquid-film” states. Sebastián [36] dehydrogenated decalin to naphthalene over 4% Pt on carbon catalyst yielding a 60% conversion. Dehydrogenation of decalin proceeded already at 200 °C when the thin film was super-heated and hydrogen produced diffused to the gas phase through the thin organic liquid and adsorbed aromatics were removed during drying step to prevent site blocking. Dehydrogenation of decalin in gaseous phase proceeds most efficiently at 377 °C.

Okada et al. [23] developed an efficient catalyst for dehydrogenation of MCH with a conversion > 95% and toluene selectivity > 99.9% under 320 °C. Liquid hourly space velocity (LHSV) was 2.0 h⁻¹ and co-feed hydrogen was 5–20 mol%. The catalytic activity was increased and sites for the cleavage reaction were reduced. The dispersion of the Pt was increased by using a pore controlled γ -alumina carrier for impregnation of chloroplatinic acid. The alkali metal species were used for masking the acid sites. The pH value was adjusted to 2.0 before

immersion of Pt (0.6 wt%). Potassium nitrate precursor was used in impregnation to achieve potassium content of 0.1 wt%.

In the 1970's, catalysts tested for the dehydrogenation of MCH included Pt/ Al_2O_3 , V_2O_5/Al_2O_3 , Co, Cu–Ni, Al–Co–Cr–Zn, Al–Cr–Mo, Ni–P, Al–Ti–V, Cr, Ru/ SiO_2 , Al–Mo–Ni [40]. In the review by Shukla et al. [41] combinations of metals for dehydrogenation of cycloalkanes covered Ni–Y-zeolites, Pt/AC, combinations with alkali reagents, Ni–Ru, Ni–Pt (40:1) on AC and partially reduced MoO_2 . Supports have included carbon materials, metal oxides, perovskites, zeolites, silica, and conductive supports like alumite (Al/ Al_2O_3/TiO_2). Good dispersion has been found for 0.25 wt% Pt/CNF and on pore controlled γ - Al_2O_3 . Metal oxide supports for Pt cover TiO_2 , La_2O_3 , CeO_2 , ZrO_2 , Fe_2O_3 , Al_2O_3 , MnO_2 , $LaNiO_3$, perovskite type oxides, and Pt/ $La_{0.7}Y_{0.3}NiO_3$. Reduced MoO_2 is also effective. Bourane et al. [16] reported that supports for dehydrogenation of MCH to **a2** have been rated in the following order: $La_2O_3 \gg TiO_2 > Al_2O_3 > MnO_2 > Fe_2O_3 > ZrO_2 > CeO_2$ [41]. The presence of bi-metallic catalysts, the metal oxide supports (under reduced conditions), and a higher metal dispersion on support and the heat of conduction of the support were found to be important [16,41]. Preuster et al. [42] referred to a study showing improved conversion of MCH to toluene by using NiZn catalyst instead of Ni-based systems.

Jensen [43] has patented dehydrogenation of cycloalkanes, for example MCH, with the Ir “pincer” complex. The dehydrogenation proceeds at about 190 °C and is reversed at about 100 °C and 10 atm or higher. Jensen and coworkers also used $IrH_2[2,6-C_6H_3-CH_2P(Bu)_2]_2$ for dehydrogenation of cycloalkanes at 100 °C when the solution was circulated through a “hot-tube” (a Pd/Ag filter tube selectively permeable to hydrogen) [44].

2.3. Benzyl and dibenzyl toluenes

2.3.1. General

Recently, dibenzyl toluenes (DBT **a6**) and benzyl toluenes (BT **a7**), common heat-transfer fluids known with trade names Marlotherm® SH (**a6**) and Marlotherm® LH (**a7**), were suggested as LOHCs. The hydrogen storage capacity of **a6** is 6.2 wt%. One cubic meter of hydrogenated **a6** stores 57 kg (624 Nm³) of hydrogen [21,24]. Prices of **a6** and **a7** are relatively low (\$4–5 per kg) and their thermal stabilities are excellent. The working temperature of DBT is in the range from 70 to 380 °C [45]. Hydrogenious GmbH has commercialized DBT as LOHC.

Müller et al. [45] studied thermophysical properties of BT and DBT. The benefit of DBT over BT is its low vapor pressure and higher boiling point (DBT 390 °C, BT 280 °C), while a lower viscosity of BT than that of DBT eases its handling (BT 2.6 mm² s⁻¹ and DBT 16.5 mm² s⁻¹ at 40 °C). Viscosity of hydrogenated H18-DBT is as high as 82 mm² s⁻¹ at 40 °C [46,47]. The enthalpies of hydrogenation and dehydrogenation of benzyl toluenes are at a reasonable range, from 62 to 71 kJ mol⁻¹ H₂. Müller et al. [45] found that the respective enthalpy is very similar for BT (–63.5 kJ mol⁻¹ H₂) and DBT (–65.4 kJ mol⁻¹ H₂). For comparison, enthalpy of hydrogenation for the N-ethylcarbazole (NEC) is from –50 to –53 kJ mol⁻¹ H₂ (Table 1). The hydrogenation of BT and DBT is enthalpically favored over hydrogenation of NEC, while hydrogen release from NEC is more favorable compared to BT and DBT.

The melting point (mp) of DBT is –48 °C and mp of its fully hydrogenated form is even lower (–58 °C). The density of DBT (1.045 g cm⁻³) is more than approximately 13% higher than the density of the respective hydrogenated form (0.921 g cm⁻³) as the aromatic rings are planar while hydrogenated rings are non-planar. The dynamic viscosity of hydrogenated BT is slightly higher than for its dehydrogenated form. The surface tension of hydrogenated DBT is lower than that for the dehydrogenated form [45].

When three aromatic rings of DBT are hydrogenated, six different hydrogenated forms may be present: H0, H6 (outer or middle ring), H12 (outer and middle ring or two outer rings) and H18 form. All of these structures have regioisomers (positions of the benzyl groups

relative to the methyl at the middle ring), and also diastereomers (chiral carbon atoms) [45,48]. Consequently, determination of the hydrogenation state of DBT is challenging using many of the analytical methods.

Aslam et al. [49] optimized reversed-phase high performance liquid chromatography method for the separation and purification of four partially hydrogenated fractions: H0-DBT, H6-DBT, H12-DBT and H18-DBT. The method used a column of phenylhexyl silica as stationary phase and 4 vol% water with 96 vol% acetone as mobile phase. Müller et al. [50] explored possibilities to define the degree of DBT hydrogenation using density, viscosity, refractive index and Raman spectroscopy. The most reliable correlations were found for density or refractive index. Uncertainty is higher for correlation using the refractive index, which decreases by about 7% during hydrogenation, than for using density that decreases by about 13%, respectively. Inhetveen et al. [51] found Raman Spectroscopy as suitable method to determine the hydrogenation rate of DBT. The setup could be automated to take samples during the manufacturing process.

Do et al. [48] used nuclear magnetic resonance (NMR) to determine degree of hydrogenation of DBT. Chemical shifts in the NMR move from the aromatic region to the aliphatic region depending on the degree of hydrogenation.

Other characteristics important for the process development for DBT have also been studied, such as the physical solubility of hydrogen in DBT [52] and binary diffusion coefficients over a temperature range from -9 to 298°C [53].

2.3.2. Hydrogenation and dehydrogenation

Brückner et al. [24] hydrogenated DBT to the corresponding mixture of perhydrogenated counterparts by using 0.25 mol% of Ru/ Al_2O_3 catalyst at 150°C and 50 bar. Conversion of BT to its H12 form was $> 99\%$ and that of DBT to its H18 form 45% in one hour.

Do et al. [48] found that the two side phenyl rings of DBT are hydrogenated prior to the middle phenyl ring. They observed that Ru on Al_2O_3 was suitable for fast side phenyl ring hydrogenation, while a make-up catalyst layer with a different catalyst material could be more suitable for the final middle ring hydrogenation.

Brückner et al. [24] found Pt/C with 1% metal loading best for the dehydrogenation of the hydrogenated DBT. More than 95% conversion of H18-DBT (**a6**) was obtained at 290°C in 210 min, while similar level of conversion of H12-BT (**a7**) was achieved at 270°C . Boiling point of **a7** was reached at that temperature and thereby higher temperatures for dehydrogenation were not studied. For **a6**, a temperature of 310°C was needed to achieve similar level of hydrogen release as for H12-NEC at 230°C .

Jorschick et al. [54] observed that the Pt on alumina catalyst (Pt 0.3 wt%, 0.015 mol%) could be used both for hydrogenation of DBT and dehydrogenation of its perhydrogenated form at 290 – 310°C by just varying the hydrogen pressure (hot pressure swing reactor). At 290°C , almost all hydrogen is released at 1.5 bar, while equilibrium shifts almost completely to hydrogenation already at 4 bar.

Amende et al. [55] studied the oxidative regeneration of Pt on alumina catalyst to remove carbonaceous residues formed over the LOHC dehydrogenation. The catalyst could be oxidative regenerated at below 327°C . Carbon dioxide and oxygenates were formed during the regeneration.

Fikrt et al. [56] studied the dynamics of a reactor system for H18-DBT dehydrogenation at above 250°C combined with a fuel cell. Hydrogen release rate could be adjusted by varying temperature and pumping rate, or by using the hydrogen buffer. Small amounts of decomposition products of DBT were observed, mainly methane, toluene, benzene, MCH and cyclohexane. Splitting of the methyl group leads to for example dibenzyl benzene, which also acts as a LOHC material. An efficiency of approximately 45% was reached for hydrogen recovery when a part of hydrogen was used for heat production. In a stationary state, the respective efficiency up to 60% could be achieved.

Terphenyls (**a8**) in partially hydrogenated form are benzene-based heat transfer fluids, however, less consistent in molecular formulation than DBT and also more expensive [57]. Completely dehydrogenated terphenyls are solid. Hydrogenation of terphenyls have been studied. Hydrogenation of the middle ring of *ortho*- and *meta*-terphenyl has been conducted using PtO_2 . Hydrogenation of middle ring has been more pronounced using copper chromite catalyst for *ortho* form than for *meta*-terphenyl. A nickel catalyst has shown preference for outer-ring reduction (referred in Ref. [48]). Sung et al. [58] found noble metal catalysts on mesoporous SiO_2 and modified carbon supports to enhance the activities of terphenyl hydrogenation and terphenyl dehydrogenation without side reactions. Pt/ SiO_2 (5%) catalyst was highly active in dehydrogenation. In terms of long-term stability, a catalyst with relatively low Pt content on the oxidized graphite coal (Sibunit-OX) was the most promising.

2.4. N-heterocyclic compounds

2.4.1. Carbazole derivatives

2.4.1.1. General. The structure of carbazole and its derivatives (Table 1) follows some of the parameters for favorable hydrogen release. N-ethyl carbazole (NEC, **b3**) with its hydrogenated form, dodecahydro-N-ethylcarbazole (H12-NEC, perhydrocarbazole), is one of the most studied LOHC pairs [18,59–63], and also recently reviewed by Crabtree [20]. This LOHC pair was first suggested by the company Air Products and Chemicals and it is patented by Pez et al. [64]. Availability of NEC **b3** from coal distillation is limited today [22], and its price is estimated to be higher than \$40 per kg. Health aspects of NEC/H₁₂-NEC is discussed in Section 5.5.

NEC has a relatively high hydrogen storage capacity (5.8 wt%). NEC is solid at room temperature (mp 69°C), though a mixture of the hydrogenated forms of NEC is liquid. To avoid the solid state, a partial dehydrogenation is suggested [65]. 90% dehydrogenation degree of the perhydrogenated NEC would yield a hydrogen storage capacity of 5.3 wt% (1.75 kWh kg^{-1}). Another solution to avoid the solid state is introducing longer alkyl chain substituents [66]. For example, the melting point of NPC is 47°C [67]. Stark et al. [67] found that the binary mixtures of NEC and NPC at eutectic composition are liquids down to 24°C with hydrogen storage capacity of 5.6 wt %. The predicted melting point for the ternary eutectic mixture of NEC–NPC–NBC was 12.6°C , whilst still offering a suitable storage capacity of 5.5 wt %.

2.4.1.2. Hydrogenation of NEC. Hydrogenation of NEC is an exothermic reaction with heat release from 50 to $53\text{ kJ mol}^{-1}\text{ H}_2$ (Table 1). Due to safety and efficiency reasons, hydrogenation of NEC is suggested in large-scale units [60,61]. Activation energy for hydrogenation of NEC over a supported Ru catalysts has been reported as 99 kJ mol^{-1} [68], 71.2 kJ mol^{-1} [69] and 58 kJ mol^{-1} [70].

Pez et al. [64] achieved fully hydrogenated NEC at 160°C and 72 atm in 250 min over a Pd catalyst. Since then NEC has been hydrogenated at 150 – 170°C and 70 bar over for example Pd, Ru and Ni catalysts [21,68–72]. Solvents are not needed for the hydrogenation of NEC, although cyclohexane has been used in some experiments [66,73] and decalin has been found to accelerate the hydrogenation of NEC [74]. Preuster et al. [42] reviewed different catalyst systems (Ni, Ru, Pt on C, C/ SiO_2 , Raney, AlO_x , $\text{TiO}_2/\text{SiO}_2$) and reaction conditions (120 – 180°C and 50–70 bar) for hydrogenation of NEC.

Eblagon et al. [70,73] found that the activity of catalysts for hydrogenation of NEC decreases in the following order: Ru > Pd > Pt > Ni. The best catalytic activity was found for 5 wt% Ru/ Al_2O_3 ($8.2 \times 10^{-6}\text{ mol NEC g}^{-1}\text{ metal s}^{-1}$) with catalytic selectivity of 98% for completely hydrogenated isomers. Rh and Pd followed Ru in hydrogenation activity regardless of the type of support.

Yang et al. [69] observed that 170°C was the optimum reaction temperature leading to complete hydrogenation of NEC over 5 wt% Ru/

Al_2O_3 in 1 h, while the higher temperatures had an unfavorable effect on reaction rate. The reaction proceeded with first-order kinetics in relation to the reactant concentration. Wan et al. [75] achieved conversion of 100% and selectivity of 98% for fully hydrogenated NEC over 1.0 gRu/g- Al_2O_3 at 60 bar, 140 °C and 600 rpm. The apparent activation energy was 27.0 kJ mol⁻¹.

Forberg et al. [76] found the bimetallic catalyst (Pd2Ru@SiCN) capable of catalysing the hydrogenation of NEC and dehydrogenation of H12-NEC. Optimal conditions for the hydrogenation of NEC were found to be 110 °C at 20 bar H_2 pressure. Forberg et al. [76] assumed that the synergistic effects of combining Pd with other transition metals is based on a lower hydride-binding energy in a metal alloy. Amorphous silicon carbonitride (SiCN) matrix offers a way to produce bimetallic nanocomposite catalysts.

Hydrogenation of NEC starts at the outer phenyl groups. H4 and H8 forms are the major intermediates in the reaction [68,70,73]. Mehranfar et al. [74] showed that H8-NEC is the main intermediate as hydrogenation proceeds through the less steric hindrance sites. H10-NEC to H12-NEC step is the rate determining step.

Sakanishi et al. [31] found that the catalysts exhibited in order of Rh > Pd > Pt > Ru for hydrogenation of acridine and carbazole at a hydrogen pressure of 70 bars and at 100–250 °C. The carbon-supported catalysts yielded products with a higher degree of hydrogenation than alumina-supported ones.

2.4.1.3. Dehydrogenation of H12-NEC. Dehydrogenation of H12-NEC is an endothermic reaction demanding heat from 50 to 53 kJ mol⁻¹ H_2 (Table 1). The activation energy of the dehydrogenation reaction is in the range of 118–127 kJ mol⁻¹ H_2 [68,77].

Adkins & Lundsted [78] dehydrogenated H12-NEC already in 1940's by using a Ni-NiCrO catalyst and benzene as a solvent with a yield of 98% at 250 °C in 1.5 h. Subsequent studies have shown that H12-NEC can be dehydrogenated at 180–260 °C at ambient pressure using Pd or Pt catalysts on alumina, silica or carbon [9,15,21,63–65,68,77,79].

Yang et al. [65] found Pd on alumina (5 wt%) as the most effective catalyst for dehydrogenation of H12-NEC at 180 °C and normal pressure. The order of the studied catalysts was Pd > Pt > Ru > Rh. The hydrogen release over Pd catalyst was 3.30 wt% in one hour and full dehydrogenation was achieved in four hours. With a Ru catalyst the maximum hydrogen release observed was 5.23 wt%. Rh catalyst was least active (4.06 wt% hydrogen released in 5 h), while it was the most selective towards the H4-NEC.

Sotoodeh et al. [80] observed that reducing the Pd particle diameter to 9 nm enhanced the dehydrogenation of H12-NEC with Pd/SiO₂ (4 wt %) catalyst. A 95% selectivity to the completely dehydrogenated NEC was obtained in 1 h, rest being the dehydrogenation intermediates. Forberg et al. [76] discovered Pd₂Ru@SiCN catalyst capable to hydrogenate NEC and to dehydrogenate H12-NEC. Dehydrogenation was completed at 180 °C in 7 h. Wang et al. [44] dehydrogenated H12-NEC with Ir based complexes of tridentate ligands (PCP pincer with two coordinating, neutral P centers and an anionic, coordinating C site) at 200 °C.

For the dehydrogenation of H12-NEC, the most stable intermediates observed have been H8-NEC and H4-NEC. Dehydrogenation started from the five-membered N-ring and then proceeding within the six-membered rings [65,68,70,71] in three stages at 128 °C, 145 °C and 178 °C [81]. Purity of hydrogen gas has been high (> 99.99%) with a trace amount of ethane (0.0029 mol%). Ten consecutive hydrogenation/dehydrogenation cycles have shown good reversibility.

Pez et al. [64] used a prototype reactor for the dehydrogenation of H12-NEC, capable of delivering hydrogen at rate of 1 g min⁻¹ to power a 1 kW engine. Peters et al. [77] developed a hydrogen release unit with the capacity of 1.75 kW_{therm}, transformed into 0.96 kW_{el} in a FC with 55% efficiency. Hydrogen output was up to 1.12 g_{H₂}·min⁻¹·g_{Pt}⁻¹ and had a power density of 4.32 kW_{el} l⁻¹. Hydrogen was released by a rate of 9.8 l·min⁻¹ (273 K, 1 bar) using H12-NEC flow of 30 ml·min⁻¹ and

temperature of 250 °C. The total reactor volume was 250 ml.

Undesired C-N bond scission at elevated temperatures has been observed for dehydrogenation of H12-NEC, leading to formation of ethane and carbazole [66,71]. However, dealkylation of H12-NEC was less than 2% in 72 h at 270 °C using a Pt on alumina catalyst [66]. Brückner et al. [24] recommended a maximum temperature of 230 °C for the dehydrogenation of H12-NEC.

2.4.1.4. N-propyl carbazole, N-butyl carbazole. Melting points of N-propylcarbazole (NPC **b4**) and butyl carbazoles (NBC **b5**) are lower than those for solid NEC (**b3**). The activation barrier for hydrogenation of **b4** with Ru catalysts is lower than that for NEC [66]. Yang et al. [82] achieved complete hydrogenation of **b4** over a Ru catalyst at 120–150 °C in one hour. The apparent activation energy was 18.4 kJ mol⁻¹. Gleichweit et al. [66] observed that the dealkylation process was most pronounced for **b3** and least pronounced for **b5**. Choi et al. [83] studied physical properties and thermodynamic efficiencies of **b3**, **b4** and n-acetyl carbazole (**b7**) and concluded **b7** as the best amongst these LOHC candidates as regards the exergy efficiencies of the hydrogen storage processes. We note that **b7** is solid.

2.4.2. Pyridines and quinolines

2.4.2.1. General. Pyridines consists of one and quinolines of two fused six-membered rings with one nitrogen atom. Hydrodenitrification of pyridines and quinolines has been widely studied in the oil refining processes using for example Ni or Co based catalysts [84,85]. The hydrogenation and dehydrogenation of pyridines and quinolines without removal of nitrogen have also been studied for syntheses of pharmaceutical compounds. Pyridine (**c1**) and its hydrogenated form piperidine are volatile and flammable and thus not favourable LOHCs. More promising LOHCs are higher boiling quinoline (**c10**) and its derivatives. Quinoline is colorless, hygroscopic and degradable liquid. Also compounds with three fused rings could be considered, for example the hydrogenated form of 4,7-phenanthroline has been dehydrogenated at below 250 °C [15]. However, we note that these compounds are typically solids at room temperature. Recently, Oh et al. [86] studied reversible hydrogenation/dehydrogenation of 2-(N-methylbenzyl)pyridine (MBP **c17**) that can store 6.15 wt% of hydrogen. MBP and its hydrogenated form (H12-MBP) are liquids. Molecular structure of **c17** resembles benzyl toluenes (**a7**). Hydrogen release from H12-MBP catalysed by Pd/C is faster than that from hydrogenated **a7** catalysed by Pt/C at temperatures below 270 °C. Instead, hydrogenation of **c17** requires more catalyst (Ru/ Al_2O_3) or prolonged reaction time compared with hydrogenation of **a7**. Repeated hydrogenation/dehydrogenation cycles were possible without degradation of the **c17** and H12-MBP. Stability, handling properties, and cytotoxicity of **c17** were acceptable according to Oh et al. [86].

2.4.2.2. Hydrogenation. Hydrogenation of quinoline **c10** and its derivatives has been studied with various supported transition and noble metal catalysts, such as Au, Pd, Ni, Rh, Ru, Pt, Cu and Co supported on for example TiO₂, Al₂O₃, SiO₂, coal, hydroxyapatite (Ca₁₀(PO₄)₆(OH)₂) and poly(4-vinylpyridine). Solvents are typically used in the hydrogenation of quinolines [11,18,32,87–92].

Complete hydrogenation of quinoline to decahydroquinoline (DHQ) is challenging, because the hydrogenated intermediates, 1,2,3,4-tetrahydroquinoline (py-THQ) and 5,6,7,8-tetrahydroquinoline (bz-THQn) tend to adsorb irreversibly to the surface of the catalyst [87]. Hydrogenation of quinoline is also inhibited in the presence of pyridines [11]. Campanati et al. [87] found dihydroquinolines rather than THQ to be responsible for the catalyst deactivation. The adsorption of the reaction intermediate(s) on the active sites of catalyst is due to the aromatic ring and takes place mainly via the nitrogen electron doublet. The hydrogen capacity of THQn is only 2.9 wt%, while it is as high as 7.2% for DHQ.

For hydrogenation of quinolines to THQ, temperatures below 200 °C and pressures from 10 bar to 70 bar are sufficient. The conversion of

THQ to DHQ requires longer reaction times, higher temperatures (175–260 °C) and pressures (110–210 bar) [32,87–90]. Deactivation of catalyst may be alleviated by using strong Brønsted acids as solvents [32,88] or by using Lewis base to offer a competitive adsorption site for the intermediates [11]. Enhanced hydrogenation of quinoline has been observed with increased basicity of the catalyst support ($\text{MgO} < \text{CaO} < \text{SrO}$) [18]. THQ has been achieved even at 20 °C with cobalt oxide/cobalt nanoparticles modified by nitrogen-doped graphene layers on alumina ($\text{Co}_3\text{O}_4 - \text{Co/NGr}@-\text{Al}_2\text{O}_3$) [89]. Sánchez-Delgado et al. [91] hydrogenated quinoline with Ru nanoparticles (1–2 nm size) on basic support poly(4-vinylpyridine) (PVPy) producing selectively the 1,2,3,4-THQ at 100–120 °C and 30–40 bar. Polar solvents, such as triethylamine, and acetic acid, enhance the catalytic performance.

Completely hydrogenated quinoline or quinaldine have been achieved in some studies. DHQ was partially formed using a strong and sterically hindered Lewis base (N,N-diisopropylethylamine) and i-propanol solvent with Pd or Rh on Al_2O_3 , while Ru/ Al_2O_3 was inactive even when a Brønsted acid (acetic acid) or base (NaOH) was added [87]. Fache [92] achieved completely hydrogenated DHQ from quinolines using Rh/ Al_2O_3 catalyst and hexafluoroisopropanol solvent. Also nano-sized metal particles have enhanced hydrogenation to DHQ as the adsorption of the intermediates on the surface of the catalyst is hindered. Campanati et al. [88] used a Rh-PLC (pillared layered clay) catalyst with 2 nm metal particle size to hydrogenate quinoline to DHQ with a yield of 41.9% at 200 °C and 20 bar in 2.5 h using i-propanol as a solvent. Fan & Wu [90] hydrogenated quinoline by using a Rh/ $\text{AlO}(\text{OH})$ catalyst with a DHQ yield of 99.3% with a fresh catalyst at 125 °C and at 8 bar within 3.5 h using a substrate/catalyst mole ratio of 120:1. The selectivity to DHQ was higher in the aprotic solvent (n-hexane) than in a protic solvent (e.g. methanol). In a protic solvent, hydrogen bonds between solvent and the π electrons of the aromatic cycle may be formed. After three cycles, particle size of Rh grew to 5.2 nm and the selectivity to DHQ decreased to 71%. Hydrogenation of the substituted quinolines were also studied. DHQ has been achieved using a Ru/hydroxyapatite catalyst at 150 °C and 40 bar (ref. in Ref. [32]). Using NanoRu@hectorite, DHQ selectivity was above 99% at 100 °C and 60 bar within 3 h in cyclohexane although for the recycled catalyst the activity and the selectivity towards DHQ reduced in the study by Sun et al. [32].

Many homogenous catalysts are capable to hydrogenate (substituted) quinolines to THQs and (substituted) pyridines to piperidines, for example Rh-based catalysts $\text{Rh}(\text{PY})_3\text{Cl}_3/\text{NaBH}_4$ (one bar in DMF), $[\text{Rh}(\text{NCMe})_3\text{Cp}^*]^{2+}$, $\text{RhCl}(\text{PPh}_3)_3$ and $\text{RhHCl}(\text{PPh}_3)_3$. (ref. in Ref. [11]). THQs can be obtained also with water-soluble Ru(II) catalysts. For example $\text{RuH}_2(\eta^2\text{-H}_2)_2(\text{PCy}_3)_2$ is capable of hydrogenating the heterocyclic ring of quinolines (a water/hydrocarbon biphasic reaction, 130–170 °C, 70–110 bar) [11]. Many Ir complexes, such as $[\text{Cp}^*\text{IrCl}(\text{imino})]$ complexes, can catalyze hydrogenation and dehydrogenation of the heterocycles [93]. Manas et al. [94] used the Ir complexes to hydrogenate 2-methylquinoline (**c11**) to the THQ at 1 atm and room temperature. Fujita et al. [95] hydrogenated for example 2,6-dimethyldecahydro-1,5-naphthyridine (**c14**, 6.0 wt% hydrogen content). With the Cp^*Ir complexes perhydrogenated products were achieved with almost 100% yields at 130 °C and 70 atm within 20 h using p-xylene as a solvent.

$\text{Fe}(\text{II})$ -(PNP) pincer complexes are able to enact the acceptorless hydrogenation and dehydrogenation of quinaldine to its THQ intermediate [96]. In the presence of catalyst (3 mol %) and KOtBu (10 mol %), the N-ring of several quinoline and indoline heterocycles were hydrogenated at 80 °C and 5 atm within 24 h using tetrahydrofuran (THF) as a solvent. 2,6-dimethylpyridine (**c7**) was hydrogenated at 10 atm pressure with a 60% yield of completely hydrogenated product (5.3 wt% hydrogen storage capacity).

Many N-heterocycles can be hydrogenated using metal-free systems. A variety of bases have been hydrogenated using a Frustrated Lewis pair approach. Geier et al. [34] achieved yields of 88% and 74% of the

THQ in the hydrogenation of 2-methylquinoline and 8-methylquinoline (**c13**) with $\text{B}(\text{C}_6\text{F}_5)_3$ (5 mol%) at 50 °C. (ref. in Ref. [97]).

Zhu et al. [98] found Ru nanoparticles supported on glucose-derived carbon spheres (Ru/CSP) were effective in the hydrogenation of quinoline to DHQ with yield up to 98.2% (in water, 120 °C, 20 bar, 4 h). Respectively, for hydrogenation of methylquinolines (**c11**, **c12** and **c13**) to DHQ, conversion of 99.9% was achieved. The activity and selectivity were lower for the hydrogenation of quinoxaline (**c15**) and **c9**. The catalyst could be recycled thrice without decrease in activity and selectivity. These results are attributed to hydrogen bonding between quinoline and hydroxyl groups of the support as well as to the p-p stacking interaction between quinoline and the aromatic system of the carbon support.

Colloidal “soluble nanocatalysts” are considered as pseudo-homogeneous having advantages over their heterogeneous counterparts in terms of activity and selectivity, while recycling of homogenous catalysts is challenging [88,99].

2.4.2.3. Dehydrogenation. Adkins & Lundsted [78] dehydrogenated DHQ to quinoline **c10** with yields of 42% and 47%, and piperidine to pyridine at yield of 48% at 350 °C in 5 h by using a Ni-NiCrO catalyst and benzene as a solvent. 2,6-Dimethylpiperidine (2,6-lupetidine, **c7**) was dehydrogenated with a yield of 45% at 250 °C. Indoline was dehydrogenated with a yield of 45% at 200 °C in one hour. Piperidines tend to convert into higher molecular weight compounds during dehydrogenation.

Ir-based catalysts have been used for dehydrogenation of nitrogen containing heterocycles. Fujita et al. [95] dehydrogenated 2,6-dimethyldecahydro-1,5-naphthyridine (**c14**) completely in almost 100% yield using Ir complexes with a bipyridonate ligand at 130 °C in 20 h using p-xylene as a solvent. Jensen and coworkers dehydrogenated 4,4'-bipiperidine (**c16**) and 4-amino-methylpiperidine with the Ir-PCP pincer complex. Electron donating or conjugated substituents to piperidine ring could increase dehydrogenation [ref. in [18]]. Xiao et al. found an Ir pincer complex $[\text{Cp}^*\text{IrCl}(\text{imino})]$ to be active for dehydrogenation of, for example THQs, under 74 °C in 2,2,2-trifluoroethanol at low catalyst loadings (0.1 mol %) [ref. in [96]]. Manas et al. [94] dehydrogenated 1,2,3,4-THQ achieving a 86% yield with Ir-based catalyst at 5% loading in 24 h under reflux in chlorobenzene (135 °C) or p-xylene (145 °C).

Chakraborty et al. [96] dehydrogenated the N-heterocycles using an $\text{Fe}(\text{II})$ -(PNP)bis(phosphino)amine pincer complex. For 2,6-dimethylpiperidine, the completely dehydrogenated product was achieved with a 58% yield in the presence of catalyst (3 mol %) and KOtBu (20 mol%) in xylene reflux (140 °C) in 30 h. Partially hydrogenated quinolines and indolines were also dehydrogenated. Quinoline or pyridine derivatives did not hamper the catalysis even though they are potential ligands for Fe.

2.4.3. Pyrroles and indoles

Pyrroles (**d1**) consist of five-membered ring with one nitrogen atom and indoles (**d13**) also a fused six-membered ring (Table 1). Similarly to the pyridines and quinolines, hydrogenation/dehydrogenation studies of pyrroles are often related to the hydrodenitrogenation processes in oil refineries [84]. Pyrrole **d1** and some of its derivatives are too volatile and flammable to be regarded as LOHC candidates. Indole (**d13**) and octahydroindole pair would have 6.4 wt% hydrogen storage capacity, however, they are solids at room temperature. Hydrogenation of indoline is difficult due to coordination through the carbocyclic ring due to many occupied coordination sites. Hydrogenation is also inhibited by basic substrates, such as quinoline and pyridine. Some Rh and Ru catalysts are able to hydrogenate **d13** to indoline in the presence of a protic acid (60 °C, 30 bar, TOF 100) [11]. Indoline having two stored hydrogen atoms, was dehydrogenated already in 1940's by using Ni-NiCrO catalyst (45% yield in one hour at 200 °C in benzene) [78]. Also Pd/C and Ru/C catalysts have been used (at 110 °C) for

dehydrogenation of indoles to the corresponding indoles, as well as Rh/Al₂O₃ and Pd on hydroxyapatite catalysts [18,100].

Butyl pyrrole (BuP, **d5**), N-methylindole (**d14**, NMI) and N-ethylindole (NEI, **d15**) have been suggested as LOHC compounds [17,101]. NMI and butyl pyrrole (**d5**, BuP) are liquids in the hydrogenated and dehydrogenated forms. Hydrogen storage capacity of NEI **d15** is 5.23 wt%. For NMI (**d14**), the hydrogen storage capacity is 5.81 wt%, but reduced to 2.88 wt%, if only heterocyclic ring is hydrogenated. BuP (**d5**) has hydrogen storage capacity of 3.14 wt%.

Hydrogenation of NEI has been conducted over a 5 wt% Ru/Al₂O₃ catalyst at 160–190 °C and at 90 bar in the presence of hexane. The hydrogenation proceeded through H₂-NEI and H₄-NEI to H₈-NEI in 4 h at 160 °C and in 1.3 h at 190 °C. No kinetically stable intermediates were produced. The apparent activation energy of NEI hydrogenation was 62.4 kJ mol⁻¹. Dehydrogenation of H₈-NEI proceeded at 160–190 °C over a Pd/Al₂O₃ catalyst, and was complete in 9 h at 180 °C (96% 4 h 190 °C). H₂-NEI and H₄-NEI intermediates were detected, the latter being kinetically stable. The apparent activation energy of H₈-NEI dehydrogenation was 117.7 kJ mol⁻¹. Purity of hydrogen was high with only a trace amount of water [17,101].

Homogenous catalysts have been studied for hydrogenation/dehydrogenation of pyrroles and indoles. Jensen et al. [17] discovered that the Ir PCP “pincer” complex, IrH₂{2,6-C₆H₃-CH₂P(But)₂}, catalyzed dehydrogenation of 5-membered ring of the hydrogenated forms of **d5** (BuP), **d14**, (NMI), indolizine (**d18**, IZ) and NEC, while activities on the 6-membered rings were modest. Dehydrogenation of H₄-BuP completed in 18 h at 140 °C, while higher temperatures (160 °C and 180 °C) were needed for H₈-NMI and H₁₂-NEC. With 25 cycles of re-/dehydrogenation no degradation was observed during 1 million catalytic TON. The Ir PCP catalyst at 100 ppm loading was estimated to represent a cost of \$5 per liter of LOHC. Hydrogenation rate of 89% for NMI (**d14**) was achieved, and further work was planned by using a 100 ppm of Pd/C in addition to a pincer complex. Brayton & Jensen [102] found the fastest dehydrogenation rate, the highest activation energy and the effective collision frequency for BuP (**d5**), which has less steric hindrance than the two ring systems. Dehydrogenation reactions were run with 1 mol% of Ir pincer catalyst at 140–200 °C in 0–48 h without a solvent. Water-soluble Ru(II) catalyst with various ligands, for example (RuH₂(η²-H₂)₂(PCy₃)₂), has been capable to hydrogenate heterocyclic ring of indole (similarly to quinoline) in water/hydrocarbon biphasic reaction at 130–170 °C and 70–110 bar [11].

Cui et al. [103] found attaching electron donating or conjugated substituents to the piperidine ring to be favourable for catalytic dehydrogenation. The highest dehydrogenation rates were observed for 4-aminopiperidine and piperidine-4-carboxamide. Undesired side reactions in hydrogenation and/or dehydrogenation were observed for 4-dimethylaminopiperidine, 4-alkoxy and 4-amino indoles and 4-aminopiperidine. We note that many of these compounds are solids.

Araujo et al. [104] found some of the nitrogen-containing compounds, for example piperazine and 1,4-dihydroimidazo [4,5-d]imidazole, promising for organic fuel cells based on their open circuit potentials (OCV). Crabtree [20] referred to possibility of using a direct fuel cell to dehydrogenate the N-containing LOHCs. For example, Driscoll [105] dehydrogenated indoline and benzyllaniline using ferrocene and quinone derivatives in catalysis, and dehydrogenation of H₁₂-NEC was also attempted. This approach would eliminate use of co-solvents and electrolytes in PEM fuel cells.

3. Solid hydrogen carriers

3.1. Solid materials by physisorption

Hydrogen can be stored in solid materials by adsorption in metals and high surface area adsorbents, or by forming a chemical bond in metal hydrides. However, low temperatures or high pressures are essential to store hydrogen by physisorption, while elevated temperatures

are needed to release hydrogen stored by chemisorption. Solid systems would require a new infrastructure as the present system is designed for liquid fuels.

For hydrogen storage by physisorption, zeolites, covalent organic frameworks (COFs), polymers of intrinsic microporosity (PIMs), hyper-cross-linked polymers (HCPs), metal organic frameworks (MOFs), carbon based materials and clathrate hydrates have been considered. Physisorption of hydrogen is based mainly on the weak van der Waals interactions between hydrogen molecules and adsorbents. Consequently, high storage capacities are achieved only at low temperatures and at high pressures. The advantages of physisorption are fast kinetics, reversibility and the relatively small amount of heat produced on hydrogen loading and high purity of hydrogen. The hydrogen storage capacity of physisorption materials correlates with specific surface area. For carbon supports, 1 wt% increase in hydrogen storage capacity requires 500 g m⁻² of specific surface area (“Chahine's rule”). Increasing the pore volume and surface area are key targets in improving the hydrogen storage capabilities of the physisorption media [63]. A few examples of the characteristics of solid hydrogen storages by physisorption are as follows:

- Hydrogen storage capacities of zeolites are low, for example max. 2.1 wt% at –196 °C and 16 bar for Na-LEV, H-OFF, Na-MAZ and Li-ABW. Zeolites are microporous aluminosilicate minerals, for example low silica type X zeolites (LSX) with alkali-metal cations (Li, Na and K) or the ion-exchanged zeolite-Y with organic ions (e.g. pyridine hydrochloride) [63].
- PIMs have generally low hydrogen storage capacity below 2.7 wt% at –196 °C and 10 bar. Hydrogen storage capacities of HCPs can be 3.7 wt% at –196 °C and 15 bar, and for COF -102 7.2 wt% at –196 °C and at 70 bar [63].
- For MOFs, hydrogen storage capacity can be high: 7.0 wt% for NOTT-122 at –196 °C and 35–40 bar, and 16.4 wt% for NU-100 at –196 °C and at 70 bar. MOFs typically contain ZnO structures bridged with benzene rings (ref. in Refs. [106] and [63]).
- 2.7 wt% of hydrogen can be stored with carbon nanotubes and nanofibers at 500 bar. An activated carbon AX-21 can store 5 wt% of hydrogen, and a zeolite-like carbon material 6.9 wt%, both at –196 °C and 20 bar. Carbon nanostructures, graphene, activated carbon, carbon aerogels and fullerenes require low temperature for hydrogen storage, but kinetics can be fast. (ref. in Refs. [5,63]). With methal-doping (for example with Sc), carbon nanostructures (e.g. organometallic fullerenes) could reversibly store close to 9 wt% of hydrogen [16].

For physisorption materials, hydrogen storage capacity can be improved by physical mixing, chemical doping, ultrasonication and by exposure of metal sites and hydrogen spillover. When a ligand is removed from the framework, the metal site is being exposed for hydrogen binding. Hydrogen spillover involves the dissociation of hydrogen onto a metal surface and hydrogen spilling over to the porous material with the aid of a catalyst [107]. The development is ongoing with reactive hydride composites, nanoconfinement of hydrides by nanoscaffold materials, synthesis of new generation alkali-alkaline earth metal composite structures and air stable nanocomposite system [108].

3.2. Metal hydrides

Hydrogen can be adsorbed in and desorbed from metals and metal alloys, but harsh reaction conditions are typically required. In addition, reaction can be slow and often it is not reversible under mild conditions. Practical hydrogen content of metal hydrides tends to be low when compared to the theoretical capacity, particularly near the room temperature. Material handling, pyrophoricity, exposure to air humidity and contaminants needs attention [16] and metal hydrides may

also be sensitive towards oxygen and water (ref. in Ref. [63]). Metal hydrides cover simple hydrides (MgH_2), alanates (NaAlH_4 , Na_3AlH_6 , LiAlH_4), borohydrides (NaBH_4 and LiBH_4), transition metal hydrides and complex hydrides. Some of these materials have been demonstrated. The following findings have been reported for metal hydrides [63,106,109]:

- Theoretically LiH can store 12.7 wt% hydrogen, but dehydrogenation temperature is 680 °C.
- MgH_2 can store 7.6 wt% of hydrogen, but dehydrogenation is slow even at 300 °C at 10 bar. Some hydride slurries are pumpable. The MgH_2 or LiH slurries can release hydrogen through a reaction with water [5]. Hydrogen could be released from mixture of MgH_2 and LiBH_4 already below 150 °C [110]. The LiBH_4 – LiNH_2 system and NaBH_4 – $\text{Mg}(\text{OH})_2$ have also been suggested [63].
- Lithium borohydride, LiBH_4 can store 18 wt% hydrogen with reasonable release temperature (appr. 280 °C), but its rehydrogenation is demanding (600 °C, 850 bar). LiBH_4 catalyzed with SiO_2 has released 13.5 wt% of hydrogen at 200–350 °C (ref. in Ref. [7]).
- NaBH_4 with water (“Millennium cell”) is proposed for FC vehicles. $\text{Be}(\text{BH}_4)_2$ stores 20.7 wt% of hydrogen, but it is toxic and expensive. Other borohydrides are for example CaBH_4 and MgBH_4 .
- Alanate LiAlH_4 can store 10.6 wt% hydrogen, of which 5.3 wt% is released at 175–220 °C, and the rest at 370–483 °C. NaAlH_4 doped with CeB_6 can store reversibly hydrogen up to 5 wt% at 75 °C. NaAlH_4 is used as a hydrogen carrier for proton exchange membrane (PEM) fuel cells. Alanates considered are also $\text{Mg}(\text{AlH}_4)_2$ and the mixed species such as $\text{Na}_2\text{LiAlH}_6$.
- Mg_2FeH_6 can store 5.5 wt% hydrogen with hydrogen release at 320 °C.
- Hydrogenated lithium nitride (Li_3N) can store theoretically 10.4 wt% of hydrogen, and practically 6.5 wt% with reversible reaction at above 320 °C and at 100 bar.
- Mixed systems, such as Li–N–H with Mg can store hydrogen up to 9.1 wt% with hydrogen release below 200 °C at 100 bar.
- $\text{Mg}(\text{NH}_2)_2$ can theoretically store 7.1 wt% of hydrogen, but its complete release is challenging.
- Complicated systems are also studied, for example THF-containing binary-clathrate hydrates [109,111].
- Hydrides based on heavy elements (e.g. Ti, Fe, Zr, Mn, La and Ni) have modest hydrogen storage capacities (below 4 wt% for LaNi_5 or Ti–Fe) [112].

The rate of hydrogenation and dehydrogenation of metal hydrides can be improved by ball milling, nanostructuring, thin films, doping the metal substrate, by the use of catalysts and additives and by changing thermodynamic parameters [63,106,109]. Hydrides have been recently reviewed by Niaz et al. [113].

3.3. Boranes

One of the extensively studied hydrogen storage materials is ammonia borane (NH_3BH_3 , AB), which can theoretically contain up to 19.6 wt% hydrogen (practically up to 16 wt%). Melting point of AB is 112–114 °C, but its slow decomposition starts already at 70 °C. In dehydrogenation, 6.5 wt-% hydrogen is released (BH_3NH_3 (l) \rightarrow H_2BNH_2 (s) + H_2 (g), $T_i \sim 137$ °C) and a polymeric polyaminoborane (BH_2NH_2)_n is followed by borazine ($\text{B}_3\text{N}_3\text{H}_6$), and finally, a boron nitride (BN) at 450 °C [114]. Regeneration of AB is challenging. The catalytic AB rehydrogenation gives a mixture of $\text{BH}_3\text{NH}_2\text{BH}_2\text{NH}_3$, (H_2NBH_2)_n (n = 3.5), (HBNH)₃ or (HBNH)_n [7]. 10% water solution of AB loses 1.8% of hydrogen in four days and 4.8% in a month when stored at ambient temperature. AB is soluble in water (26 wt%) and methanol (23 wt%), and slightly soluble in ethyl ether, hexane and benzene at room temperature. Purity of hydrogen released from AB is over 99% [114].

Ball milling and use of platinum salts increase hydrogen release from AB at lower temperatures. Some hybrid materials with hydrides, MOFs, graphene and carbon cryogels enable a hydrogen release already at 50 °C. Doping with diammoniate of diborane ($[(\text{NH}_3)_2\text{BH}_2]^+[\text{BH}_4]^-$) or ammonium chloride in THF improved the hydrogen release of AB to 14 wt% at 40 °C. Also ionic liquid media and catalysts have shown positive effect on the decomposition of AB [63].

From amidoboranes and ammonia complexes $\text{M}(\text{BH}_4)_n\cdot m\text{NH}_3$ (M = Li, Al, Zn, Ca, Mg, Y), a mixture of $\text{Mg}(\text{BH}_4)_2\cdot 2\text{NH}_3$, LiNO_3 , and PTFE provides appr. 12.5 wt% hydrogen in pellets with good stability up to 75 °C [114,115]. Hydrogen can be released from a combination of $\text{Mg}(\text{BH}_4)_2\cdot 2\text{NH}_3$ and LiAlH_4 at 100 °C [115]. Hydrazine borane ($\text{N}_2\text{H}_4\text{BH}_3$) with LiH uptakes 14.8 wt% hydrogen, of which 11 wt% can be released at 150 °C within one hour [63].

4. Circular hydrogen carriers

4.1. Methanol, hydrocarbons and formic acid

Carbon-neutral cycle is achieved by producing methanol, methane or liquid hydrocarbons from renewable hydrogen and CO_2 extracted from fuel gas or atmosphere (Fig. 3) and by using these circular fuels for ICEs, turbines, FCs, or for further synthesis of chemicals.

Fossil natural gas (methane CH_4) is a common fuel representing 22.6% (appr. 3063 Mtoe) of the world TPES in 2013 [116]. Methane is the major constituent in biogas, and it can also be produced through gasification from coal or biomass. Hydrogen content of methane is high, 25 wt%, and thus NG is the major source of industrial hydrogen. Methane can be reformed in small-scale, for example on-board vehicles or in refueling stations. Worldwide, approximately 100 refueling stations produce hydrogen from NG, mainly in Germany, the US and Japan [112]. Building up a new infrastructure for gaseous fuels is expensive, however, NG infrastructure already exists in many regions. A recent review by Gahleitner [117] evaluated power-to-gas pilot plants, from which 41 were realised and seven planned.

Methanol (CH_3OH) is today produced mainly from fossil NG and coal via synthesis gas (CO and H_2) at global capacity of about 95 Mt [118]. Green methanol is also produced, for example in Iceland from CO_2 present in geothermal steam and renewable hydrogen from water electrolysis (CuO and ZnO catalysts at 250 °C and 100 atm) by Carbon Recycling International (CRI) [119]. Kothandaraman et al. [120] published a system capable to capture atmospheric CO_2 using pentaethylenhexamine and reducing it with hydrogen to methanol in the presence of a Ru–Macho–BH catalysts in a solvent (initial TOF = 70 h^{-1} at 145 °C, 50 atm; in 55 h, 79% of the hydrogen was converted to methanol). Methanol is used mainly for the production of formaldehyde [121], but it can also be used as a fuel in ICEs, turbines and FCs. Methanol can be reformed into H_2 and CO for use in a PEM, or it can be used in the direct methanol fuel cell (DMFC). Methanol is used as a marine fuel in ICEs by Stena Lines [122] in Sweden and on seven ocean going ships [123]. In China, approximately 8% of motor fuel pool is methanol. Methanol is liquid, and it can be distributed through the existing fuel infrastructure with minor modifications. Hydrogen content of methanol is relatively high (12.5 wt%) and hydrogen can be released from methanol by steam reforming using elevated pressure (20 bar) and temperature (250–350 °C) in the presence of a catalyst (utilised for larger, non-mobile units) [112]. Methanol steam reforming catalyst are based on Cu, Pd, and Pt (for example Cu–Zn/ Al_2O_3) [124] and reaction enthalpy (ΔH°_R) is 49.2 kJ mol^{-1} . Homogenous catalysts enable methanol reforming under relatively mild conditions, for example Ru pincer complex (1.6 ppm in methanolic NaOH, TOF 4719 h^{-1}) [63] and Ru, Rh, Ir and Fe catalysts [125]. Methanol reforming generated hydrogen for Daimlers Ncar 5 FC demonstration vehicle [112].

Fossil fuels used today are mainly liquid hydrocarbons (HCs). Chemically similar hydrocarbons can be produced from renewable sources, for example from biomass using gasification and Fischer-

Tropsch liquefaction, or from renewable hydrogen and CO₂. These circular liquid hydrocarbons are “drop-in” options that be easily used even in the most demanding sectors, such as aviation [126].

Many analyses have been carried out to evaluate technological and economical feasibility of synthetic methane, methanol or hydrocarbons. For example Hannula [126] found production of methane most economical, followed by methanol and then hydrocarbons (gasoline). However, the infrastructure needs of using gaseous methane were not considered. Tremel et al. [127] found methanol production more feasible than production of Fischer–Tropsch hydrocarbons or methane when techno-economic parameters and the public acceptance were considered. Fischer–Tropsch route was expected to have the highest public acceptance. Methane suffered from low product price of natural gas when economy was evaluated based on the ratio of market price to potential production costs. For methanol, market price of high value ethanol was used.

Storing hydrogen is possible also by using formic acid (HCOOH) synthesized from hydrogen and CO₂, and by its catalytic decomposition to hydrogen and CO₂ under mild conditions. Gravimetric hydrogen capacity of formic acid is 4.4 wt% and its volumetric hydrogen capacity is 52 g L⁻¹. Homogenous Rh-, Ru- and Ir-based catalysts have been studied for the hydrogenation of CO₂ in water or in DMSO, for example [Cp*Ir(dhbp)Cl]⁺ and the [RuCl₂(PTA)₂]. Hydrogen has been released from formic acid by using catalysts based on for example Au, Pd, Ir, Pt and Rh on carbon or alumina. Also TiO₂, CdS, Pd–Au/C, Pd–Ag/C, Au/TiO₂, and Au–Pd/MOF catalysts have been active. Nanosized Au/Al₂O₃ has shown high activity without formation of CO as a by-product. PdAu@Au core-shell nanoparticles supported on AC have been more active than the Au/C and Pd/C. Ultrafine Pd nanoparticles on graphene oxide (Pd/PDA-rGO) exhibited the TOF of 3810 h⁻¹ at 50 °C. Hydrogen release from formic acid has also been studied using homogeneous Rh-, Ru-, Ir- and Fe-based systems, such as IrH₂Cl(PPh₃)₃ and RhCl₂(PPh₃)₃. Ru(H₂O)₆ or RuCl₃·H₂O combined with mTPPTS ligand and HCOONa additive in an aqueous solution showed no deactivation of catalyst over 100 cycles at 90 °C. In addition, no CO by-product was detected. One of the Fe-based catalysts achieved TOF of 9425 h⁻¹ at 80 °C [18,63].

4.2. Ammonia and its derivatives

4.2.1. Ammonia

Ammonia is produced by using energy intensive Haber–Bosch process, and it is one of the largest chemicals. A global production capacity of ammonia was over 140 Mt in early 2000's with cost of \$136 per tonne [128,129]. Major part of produced ammonia is used for synthesis of fertilizers and it is found in home cleaning solutions. Ammonia is used in the Selective catalytic reduction (SCR) systems to reduce nitrogen oxide (NO_x) emissions from industrial plants, and in a form of urea or ammonia formate from transport applications [130]. Ammonia can be used in the alkaline fuel cells (AFCs), which operate in the temperature range of 10–66 °C without need for shift converter, selective oxidizer or co-reactants such as water. No final hydrogen purification stage is needed [114]. Technology for transportation, distribution, storage and utilization of ammonia is available, but its toxicity, flammability, corrosiveness and pungent odour arises safety concerns [131]. A typical industrial grade ammonia contains appr. 27 wt% of ammonia and 73 wt% of water so that it can be safely transported. Ammonia's toxicity and adverse health effects can be mitigated also by its conversion into solid urea, ammonium formate, carbamate salts and metal amines (see the following Sections).

Hydrogen content of anhydrous ammonia is high, 17.8 wt-%. According to Raissi [114], 16% of the energy stored in ammonia is needed to decompose ammonia into nitrogen and hydrogen. Dissociation of ammonia with Ni catalyst requires temperatures above 1000 °C. The nitrided MoN_x and NiMoN_x on α-Al₂O₃ are active for ammonia (NH₃) dissociation at 650 °C with conversion of over 99%. This

temperature is lower than required for the commercial 10 wt% Ni on alumina, Fe–Co or NiO on alumina catalyst. Ru and Ir based catalysts have been capable to dehydrogenate ammonia under mild conditions. Also transition metal nitrides and carbides, such as Mo₂N, VN, and VC_x, have been tested, and alloys such as Fe–Al–K, Fe–Cr, La–Ni (–Pt) and La–Co (–Pt) [114].

Besides the large NH₃ crackers (up to 1.2 MW), NH₃ dissociators are developed for smaller applications (150 W). A system utilizing the microchannel reaction technology with estimated costs of \$300 has been developed for the hydrogen generator and from \$10 to \$20 for each ammonia canister delivering about 60 g of H₂. Larger NH₃ crackers may have the overall efficiency as high as 85%, while smaller NH₃ crackers have efficiency of appr. 60% [114].

4.2.2. Ammonium metal complexes

Ammonia can be reversibly stored in the solid ammonium metal complexes. When heated, ammonia coordinated to the central metal cation is released. The absorption of ammonia in metal complexes is exothermic and its desorption is endothermic [132]. Commercial cartridges of ammonium metal complexes are available from Amminex (AdAmmine™) (<http://www.amminex.com>).

Dihalo ammonium metal complexes have structure M(NH₃)_nX₂, where M = Li, Na, Mg, Ca or transition metal, X = halide and n = 1–8. Magnesium ammonium chloride, Mg(NH₃)₆Cl₂, can store 9.7 wt% hydrogen, while Ca(NH₃)₈Cl₂ can store 8.5 wt% hydrogen [133]. For Mg(NH₃)₆Cl₂, four ammonia molecules are released at temperature below 100 °C, and the last two ammonia molecules below 300 °C. Ca and Sr ammonium complexes start to release ammonia already at room temperature.

Ammonia can be absorbed in MgCl₂ powder (99%) at 6.7 bars and 171 °C in 9 h, but absorption time can be shortened into minutes at elevated pressure. Ca and Sr ammonium chlorides have vapor pressures of several bars at below 80 °C and nearly 0.5 bar at room temperature [132]. We note that when using chlorides, risk for formation of corrosive HCl in contact with water deserves consideration.

4.2.3. Ammonium carbamate and carbonate

Ammonium carbamate (H₂NCOONH₄) and ammonium carbonate ((NH₄)₂CO₃) decompose completely into NH₃ and CO₂ at temperatures between 30 °C and 85 °C. Carbamate decomposes completely at 60 °C, and it provides higher gravimetric ammonia yield than carbonate. The carbonate generates ammonium bicarbonate as a stable intermediate and water as a by-product. Ammonium carbamate may form carbamic acid as an unstable intermediate and urea as a by-product. Upon heating and cooling a mixture of ammonium carbamate, ammonium carbonate, intermediates and by-products may be achieved regardless of the salt used initially. Upon cooling, the process reverses to the original ammonium salt. A minimum temperature from 70 to 80 °C is needed to prevent formation of solid ammonium carbamate. Vapor pressure of ammonium carbamate is 82 mbar and that of ammonium carbonate is 69 mbar at room temperature. In an open container, they will slowly sublime. Chamber pressure stays below 6 bar in a sealed stainless steel vessel. Ammonium carbamate seems a better ammonia precursor than ammonium carbonate as it decomposes easily, generates the higher ammonia pressure, and does not form water [132].

4.2.4. Urea and ammonium formate

Urea (CO(NH₂)₂) is produced from ammonium carbamate, and it is primarily used as an agricultural fertilizer, and in the food processing industry. The use of urea in the SCR systems in diesel engines represents a few percents of its consumption. Global production capacity of urea was 133 Mt annually in early 2000's [130].

Urea solution commonly used as ammonia source in SCR consists of 32.5% of urea and 67.5% of deionized water (ISO 22241, tradename AdBlue). 1 kg of the 32.5% urea solution is equivalent to 0.184 kg of ammonia. At concentration of 32.5 wt%, urea forms a eutectic solution

with the lowest crystallization point of $-11\text{ }^{\circ}\text{C}$ (solubility in water is 50%). Urea solutions of higher concentrations have been used for marine and stationary engines. The urea solution is clear, non-toxic and safe to handle, albeit it can corrode some metals and damage the aquatic environment [134]. AdBlue has the pH in the range of 9.0–9.5 [135]. Urea decomposes to NH_3 and CO_2 at appr. $160\text{--}290\text{ }^{\circ}\text{C}$, but its hydrolysis may be only partly completed even at higher temperature. Decomposition of urea proceeds through two reaction steps, involving an isocyanic acid (HNCO) intermediate and possible, undesired byproducts including cyanuric acid $\text{C}_3\text{N}_3(\text{OH})_3$, biuret $\text{H}_2\text{NC}(\text{O})\text{NHC}(\text{O})\text{NH}_2$, and melamine [136,137].

A mixture of urea, ammonium formate (HCOONH_4) and water is sold with a trademark “Denoxium”, developed by Kemira in 2004. A 40% water solution of ammonium formate has a freezing point of $-35\text{ }^{\circ}\text{C}$. Ammonium formate decomposes into ammonia and byproducts when heated. The ammonia content in ammonium formate is lower than that in urea [137].

5. Discussion

5.1. Criteria for hydrogen storage media

Hydrogen could serve the storage needs of renewable energy, complementing the existing energy storages in a flexible manner. Hydrogen as an energy carrier is interesting for example in long-distance and inter-continental transportation, off-grid and remote locations, and in daily, seasonal and long-term reserves.

Some of the desired characteristics for hydrogen storage media are application-dependent, while some of the requirements are similar regardless of their use. Generally, material should be capable of storing hydrogen at near ambient temperature and at normal pressure without losses [15]. The technical criteria for hydrogen storage media are more demanding for transport applications than for power plants and ships, while the economy is particularly challenging in the sectors accustomed to the low-cost fuels. Road-transport is one of the most demanding sectors due to the dynamic hydrogen need in transient driving conditions. The U.S. Department of Energy (US DOE) has defined targets for hydrogen storage media based on the needs of road transport (see Supplementary material). Examples of the 2020 targets are: system capacity of hydrogen in minimum 5.5 wt% (1.8 kWh kg^{-1}) and 40 kg m^{-3} (1.3 kWh L^{-1}), and hydrogen loss rate in maximum 0.05 kg kg^{-1} .

The different aspects of hydrogen storage options have been discussed, for example by Crabtree [7,20] and David [138]. Generally, hydrogen storage media should have sufficient energy density, stability, operability, kinetics, quality of hydrogen (particularly for FCs), infrastructure, the capability for long-term storage at different size classes, safety, biodegradability, life cycle durability, maturity of technologies, economy and scalability. However, there are differences in criteria between user sectors, and consequently several hydrogen storage solutions are necessary.

5.2. Storage sizes and times

Storing hydrogen as compressed or liquefied is feasible for relatively large storages and for limited storage times, for example from 100 kWh (pressurized tanks) to 100 GWh (cryogenic storage) [5]. For stationary uses, hydrogen can be stored in ground storages (old salt mines, gas fields, caves), in pressure vessels, or as a liquid in “Dewar” systems [6]. Storing hydrogen on a small scale and for long time periods is limited due to hydrogen losses.

Solid hydrogen storage is not compatible with the existing infrastructure, and there are also other challenges related to the high pressures or severe temperatures needed in the hydrogenation and dehydrogenation cycles.

Hydrogen storage sizes and times are not limited for the LOHC

concept, and hydrogen is not lost in standard conditions; large- and small-scale, as well as short- and long-term storage is feasible (similar to diesel fuel). Hydrogenious GmbH offers LOHC systems in the size classes from 30 kW to 1 MW input power (up to $1500\text{ Nm}^3\text{ h}^{-1}$ or 135 kg h^{-1} of hydrogen) and with a storage capacity from 10 MWh to 1 GWh, and selection is expanding [21].

Storage sizes and times for gaseous fuels are restricted in general, and this applies also to circular methane. Instead, circular methanol is a liquid fuel resembling gasoline, and thus suitable for all storage sizes and times. This is also valid for other circular liquid compounds. Ammonia is also liquid, but it is burdened with safety related limitations (if not converted to safer forms).

5.3. Energy densities

The volumetric energy content of hydrogen is low at standard temperature and pressure (0.0108 MJ L^{-1}) and even when compressed at 700 bar (5.0 MJ L^{-1} , 40 g L^{-1}) or liquefied at $-253\text{ }^{\circ}\text{C}$ (8.5 MJ L^{-1} , 70 g L^{-1}). A slightly higher energy density is achieved for cryo-compressed hydrogen (pressurized liquefied hydrogen), namely 80 g L^{-1} at 300 bar for a prototype developed by BMW and Linde [139]. Compared to hydrogen, the volumetric energy content of gasoline is superior (32.6 MJ L^{-1}), while the gravimetric energy content of hydrogen (120 MJ kg^{-1}) is theoretically almost three times higher than that of gasoline (43 MJ kg^{-1}). However, the real gravimetric energy content of hydrogen may be modest when the total system is taken into account (depending on the size and type of containers). For example, the storage capacity of compressed or liquid hydrogen is typically below 7.5 wt% (9 MJ kg^{-1}): system weight for 3 kg hydrogen at 700 bar is 50 kg (100 l), at 350 bar 45 kg (145 l) and at 1 bar and $-253\text{ }^{\circ}\text{C}$ is 40 kg (90 l). The practical maximum of the gravimetric storage capacity of hydrogen is estimated as 20 wt% [140]. Furthermore, losses of hydrogen reduces the practical energy density of liquid hydrogen based systems.

The hydrogen storage capacities of some solid materials are theoretically high. For example, ammonia borane can store 19.6 wt% hydrogen, but regeneration of material is difficult. Metal hydrides can store more than 8 wt% (90 g L^{-1}) hydrogen, but high pressures (10–60 bar) and low temperatures ($-196\text{ }^{\circ}\text{C}$) are typically required [140].

The LOHC system based on DBT has a hydrogen storage capacity of 6.2 wt% (62 g L^{-1} hydrogen, 7.4 MJ kg^{-1}). This is higher than the US DOE target of 5.5 wt% for 2020, and higher than the practical hydrogen storage capacity of compressed or liquefied hydrogen today when the system weight is taken into account. However, experience on the hydrogen content that can be released in practice from the LOHC is also needed.

The energy contents of circular hydrogen carriers are relatively high when combusted as whole, for example 50 MJ kg^{-1} (36 MJ m^{-3} $0\text{ }^{\circ}\text{C}$, 1 bar) for methane and 20 MJ kg^{-1} (15.9 MJ L^{-1}) for methanol. The hydrogen content of methane is 25 wt% and that of methanol is 12.6 wt%. Ammonia also has a high hydrogen content (17.5 wt%), but due to safety concerns it is often used in other forms (urea, ammonium salts or metal complexes) that have lower hydrogen contents [132]. All circular hydrogen carriers are irreversible, thus the material needs to be manufactured for every cycle from the beginning using CO_2 or nitrogen as building blocks, while a smaller amount of reversible LOHCs can serve larger energy needs.

The hydrogen contents of different hydrogen storage materials are illustrated in Fig. 4.

5.4. Maturity of technologies

The positive features of storing hydrogen in compressed or liquid form are the maturity of the technology and the ease of use without complex conversion technologies or reactors. Solid hydrogen storage materials are not regarded as mature technologies today.

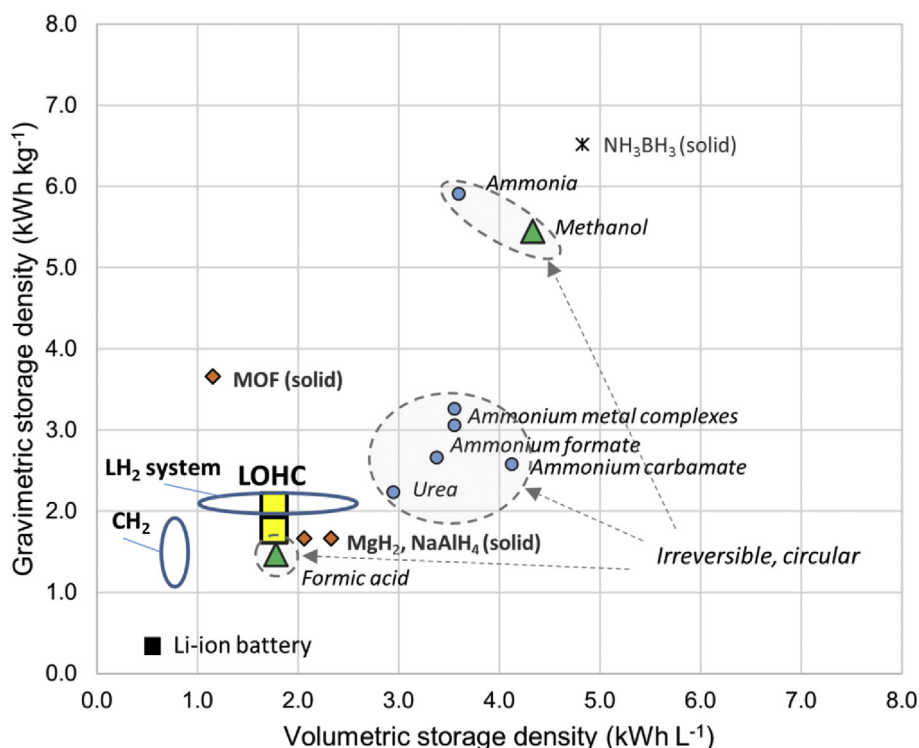


Fig. 4. Gravimetric and volumetric energy content of selected hydrogen storage candidates [3,48,63,106,132,133,140,171–174].

The LOHC technology based on DBT is already commercially available, but it is still at early phase of market introduction. Aromatics have been hydrogenated for decades in oil refineries, however, their decentralised hydrogenation at a smaller scale is neither optimised nor common technology. Dehydrogenation of cycloalkanes to aromatics is also a known technology, but again, not at a small scale. For these purposes, optimised processes and catalysts are needed, viz. robust, efficient, selective catalyst and safe operations in mild conditions. Furthermore, different chemical compounds have pros and cons as LOHCs. Hydrogen release from many heterocyclic compounds is easier than that from the respective hydrocarbons, while aromatics are typically more easily hydrogenated than their heterocyclic counterparts (Table 3) [24]. For example, an NEC/H12-NEC system would be interesting as a LOHC pair, but the solid form of NEC is a shortcoming. Many development steps are expected in chemistry and technology related to LOHCs. Also an intermediate hydrogen container may enable the use of milder reaction conditions (slower hydrogen release) while still providing sufficient hydrogen supply for transient hydrogen release needs.

Circular methane and methanol can be used in fuel cells, ICEs or turbines with existing technology and acceptable kinetics. The disadvantage of these fuels are related to the technological and economical challenges in their manufacture from renewable hydrogen and renewable or re-cycled CO₂ or nitrogen. Ammonia is used (also converted to urea, ammonium salts, or metal complexes in e.g. AdAmine™ cartridges) for several purposes, but currently not for storing hydrogen [141].

5.5. Safety and environmental aspects

While hydrogen is non-toxic, it is flammable over a wide concentration range (4–77%). The explosion range of hydrogen is 18–59 vol%. Furthermore, hydrogen leaks are difficult to detect, as odorants are not practical (different rate of leak) and hydrogen sensors are ineffective. A hydrogen molecule can diffuse through materials, cause embrittlement of metals and it can react with oxidizing elements.

Minimum ignition energy for hydrogen (0.005 mcal) is only a fraction of that of static electric discharge [3,112]. Hydrogen-oxygen flames are nearly invisible and a flame detector may be needed [112]. The auto-ignition temperature of hydrogen in air is appr. 500 °C. Temperature rises to some extent when hydrogen is released from a pressurised vessel [3]. The safety record for hydrogen is good as it is used almost solely in industry, with standardised procedures and by trained personnel. In addition, most of the hydrogen is produced on-site without the need for transport [112].

For hydrogen storage materials, safety issues are related to the hydrogen released and to the material itself. Hydrogenated forms of the LOHCs are often less familiar than their dehydrogenated counterparts. For DBT, health and safety assessments are available as it is a common heat-transfer liquid. DBT is classified as a low risk chemical with symbols N, dangerous for the environment and Xi, irritant. Also the flammability of DBT is low [21,24]. Similar safety information for the hydrogenated DBT is not available. Concerning potential heterocyclic LOHCs, Markiewicz et al. [9] observed that toxicity (a half maximal effective concentration EC50, *Daphnia magna*, water flea) for 2-methylquinoline and its hydrogenated forms was comparable to diesel fuel, while toxicity of the partially hydrogenated form resembled that of gasoline. Potential concerns of bioaccumulation were indicated for the H8-NEC. 2-methylquinoline was biodegradable, while NEC was not. Aromatics usually degrade more easily than cycloalkanes, and paraffins more easily than olefins. Zhang [142] found a quinaldine-based LOHC system to show no or only a slight toxicity toward soil bacteria. As referred to by Crabtree [20], nitrogen-containing organic molecules tend to have better biodegradability than alicyclic compounds.

Of the circular hydrogen carriers, methane and methanol are used widely and procedures for their handling are well-defined. Methane is a gas that needs special safety measures, particularly when stored in liquid form at –162 °C. Methanol can be handled similarly to gasoline, as both liquids are flammable, volatile and toxic. However, methanol is biodegradable, while gasoline is not [112,143].

Ammonia is an invisible gas that is toxic at sufficient concentrations. The National Institute of Occupational Safety and Health (NIOSH) limit

for ammonia is 25–30 ppm for long-term exposure, 300 ppm for the immediately dangerous level, and 5000 ppm for the fatal levels within minutes [132]. Ammonia may affect by direct contact with the eyes and skin or through ingestion [114]. Ammonia can be stored under appr. 26 bar. Its explosion range is 16–27 vol% at 0 °C and 1 atm. Ammonia is lighter than air. The autoignition temperature for ammonia vapour is 651 °C. Risks related to ammonia can be alleviated by using aqueous ammonia, urea, ammonium carbamate or carbonate, or metal ammonium chlorides, for example AdAmmine™ cartridges classified by the UN as non-hazardous goods [141]. For these materials, the safety concerns are related to accidental ammonia release. Fulks et al. [132] estimated the safety scenario for an ammonia leak under a car in a garage at 60 °C, with a 6 L canister at 18 bar. The main concentration of ammonia was estimated to be under the car near the leak, and the remainder of the garage was above the odor threshold, however, below the dangerous level. Safety risks related to the flammability range of ammonia were deemed as not higher than those of conventional fuels.

5.6. Infrastructure

For hydrogen transportation via pipelines, trucks and tankers, special consideration is needed. Conventional natural gas pipelines are not compatible with hydrogen, for which special steels are needed to avoid diffusion [112]. Pipelines are available for hydrogen transport for oil refineries and ammonia production plants at total length of 1500 km in Europe and 2000 km (69 bar) in the US [6].

For truck or tanker transport of hydrogen, compression or liquefaction is used. Compression consumes 6–15% of the energy contained in hydrogen [3,5,9,112]. Steel containers can be used for hydrogen at 200 bar, while composite materials are used in the cylindrical tanks at 700 bar [6]. Liquefaction and cooling consumes approximately 30% of the energy of hydrogen [3,9,112]. Furthermore, boil-off and evaporation losses are substantial. For liquid hydrogen in cars or truck transport, appr. 1–5% of the hydrogen is lost daily [5,21,144], and the daily loss is 0.3% for a tanker (4000 kg hydrogen) [5]. In some applications hydrogen losses can be minimised by using vaporized hydrogen simultaneously, however, this requires continuous operation. Long-term storage or overseas transport of hydrogen is therefore challenging.

Infrastructure for solid hydrogen storages does not currently exist.

LOHCs are compatible with the existing infrastructure for liquid fuels, and light-weight tanks can be used. LOHCs don't lose hydrogen even when transported overseas or in long-term storage under ambient temperature and pressure. A large truck (40 t) can carry 1800 kg of hydrogen in DBT-LOHC, which is a substantially higher amount than that can be transported as compressed hydrogen (400 kg at 200 bar [6], up to 1000 kg at 500 bar with tube trailer [5]). Note, a 40 t truck can carry 26 t of gasoline, which has energy equivalent to 8000 kg of hydrogen. For a hydrogen retail station delivering 200 kg hydrogen per day, hydrogen delivered in DBT-LOHC with one 40 t truck would be sufficient for nine days [5,145]. Chiyoda Corporation has the toluene based LOHC system (SPERA), which is used for overseas supply of hydrogen to a power plant in Japan. New demonstration facilities are also under construction at Chiyoda R&D Center with operation scheduled for 2018. In addition, the size of dehydrogenation unit will be reduced to serve e.g. as a refueling station for fuel cell electric vehicle (FCEV) [23,146–148].

Methane, a circular hydrogen carrier, is a gaseous fuel that requires a special infrastructure, which is, however, available in many countries. Methanol and liquid hydrocarbons are compatible with the infrastructure for liquid fuels with slight or no modifications.

5.7. End-use aspects

Requirements for hydrogen storages are less demanding in static use (in permanent locations or containers transported by trucks and ships) than in dynamic use (fuelling ICEs, FCs or turbines for buildings,

industries, vehicles, ships and machinery). There are differences in usability between hydrogen storage options. Compressed hydrogen is appropriate in a relatively small scale (below 300 kW), while liquid hydrogen can be used in a larger scale (100 MW scale) [149]. Neither of these forms is ideal for extended storage times nor dynamic use. Liquid LOHCs and circular methanol or liquid hydrocarbons are flexible options for different size classes and storage times. They don't lose hydrogen unintentionally and they are safe in standard conditions. Methanol is suitable even for the most demanding dynamic use with the existing technology. The challenge of the LOHC system is the need to dynamically release hydrogen in a reactor before its use for some applications. Direct LOHC-FC systems suggested by Ajaujo et al. [104] and others are interesting developing technologies.

Case-specific evaluations are needed to choose the most suitable hydrogen storages for different uses. Integration possibilities and the availability of waste heat will improve the total system efficiencies for the LOHC system, as well as combining the exothermic hydrogenation and endothermic dehydrogenation. According to Preuster et al. [42], at least 27% of the hydrogen is lost, if the DBT-LOHC system is not integrated to the source of excess heat. The LOHC system has already been evaluated for many industrial end-uses, for example in a micro-algae plant [150], in a wind park and in a cement plant [151], in a concentrated solar power plant [152] and for seasonal storage in a hydropower plant [149,153]. One of the end-uses suggested for the DBT-LOHC is utilising stranded gas off-shore or at remote drilling sites by converting at least 5–14% of the methane into hydrogen [154].

Safety is particularly important in the end-use applications, where users are not professionals and operations take place in public locations. Some examples of these are given below with comments on the possible LOHC use. Here the hydrogen storage capacity of LOHC is assumed to be 5.5 wt%, and the FC efficiency as 80% (today it is 43–60% without the utilisation of waste heat [5]).

- **A 55 kW FC family car** running at 60% load for 5 h (165 kWh), would use 113 kg of LOHC to provide the 6 kg hydrogen needed over appr. 500 km of operation (hydrogen consumption 1–1.5 kg per 100 km for FCV [155]). Endothermic hydrogen release would require an external heat source besides using waste heat from FC. For cars, LOHC needs to be liquid at all operating temperatures (from sub-zero to appr. 80 °C). Exothermic hydrogenation onboard a car would be challenging as substantial cooling would be needed. For automotive use, a dehydrogenation temperature of approximately 200 °C would be acceptable [14]. Toluene [25,26] and NEC based [14] LOHC systems have been evaluated for vehicles.
- **A family house** with an annual energy consumption of 5 MWh (0.33 kW), would need 3400 kg of LOHC to provide 187 kg hydrogen. The low electricity-to-electricity efficiency of the LOHC concept could be increased by utilising the waste heat of the exothermic hydrogenation for heating or cooling purposes. The waste heat of FC could also be recovered (PEM 80–180 °C, solid oxide fuel cell, SOFC, up to 600 °C). With the LOHC concept buildings could store renewable energy [60].
- **A ship with 41 MW** would consume 1 GWh over 24 h operation at full load. 680 tonnes (28 tonnes per hour) of LOHC would be needed to release 37.4 tonnes of hydrogen, which is the same respective amount as 200 tonnes of marine diesel fuel. Due to limited space on-board ships, one tank should be capable of handling both loaded and unloaded LOHC assisted by, for example, flexible walls. On-board charging of LOHC would reduce its volume needs.
- **Emission control device** to reduce NO_x from a large marine diesel engine operating at full load would need 31.9 kg h^{−1} LOHC (1.75 kg h^{−1} hydrogen) to reduce 20 kg h^{−1} of NO_x (assuming 2NO + 4H₂ + O₂ → N₂ + 4H₂O). Today, urea or ammonium formate is used for the NO_x reduction, and in some on-road applications commercial solid, reversible, ammonia cartridges are used (AdAmmine™, appr. 450 g ammonia per liter of SrCl₂) [141,156].

Table 2

Conversion efficiencies of various hydrogen based pathways starting from electricity (100%). (1) Power-to-power: H₂ stored until re-electrified (2) power-to-gas: H₂ blended in the NG grid or transformed to methane (3) power-to-hydrogen: H₂ used as such or as feedstock. Power-to-power options using LOHC are shown with present technology (4) and future technology (5).

Electrolysis	Conversion, transport, distribution, retail	Final efficiency	Reference
(1) Electrolysis (73%)	Compression (67%)	FC (29%)	[5]
(2) Electrolysis (73%)	Methanation (58%), compression (55%), distribution (54%)	Gas turbine (21%)	[5]
(3) Electrolysis (73%)	Compression CH ₂ (67%), distribution (64%), retail (54%)	FC (24%)	[5]
(4) Electrolysis (70%)	LOHC hydrogenation (69%), dehydrogenation (48%)	PEM-FC (26%) ^a	[21]
(5) Electrolysis, SOEC (90%)	LOHC hydrogenation (88%), dehydrogenation (86%)	SOFC-FC (43%) ^b	[21]

^a Waste heat < 150 °C.

^b Waste heat < 400 °C.

5.8. Efficiencies and costs

Total efficiencies are low for different hydrogen-based pathways to utilise renewable energy due to several conversion steps (Table 2) [5]. In the power-to-power option (1, hydrogen stored in large-scale until re-electrified), in the power-to-gas option (2, blended in the NG grid or transformed to methane) and in the power-to-fuel option (3, used as such), the total efficiencies are in the range of 20–30%. In the power-to-feedstock concept, hydrogen is used for example in the refining or other chemical industry. Total efficiency of the direct use of hydrogen in option 1 is higher than that of options 2 or 3. However, distribution of electricity is limited to the grid region in option 1 and thus it cannot serve all end-use sectors. In all pathways, electrolysis is energy-consuming step; currently based on alkaline or PEM technology, while more efficient high temperature solid oxide electrolyser cell (SOEC) electrolyzers are being developed. End-use efficiency depends on the technologies selected and possibilities for integration with waste heat utilisation. Energy losses in the compression of hydrogen are 6–15% and in liquefaction 30%. For liquid hydrogen, the boil-off losses should also be considered [3,5,9,112]. For methane, energy losses in conversion, transportation and distribution are estimated as approximately 19% (mainly in hydrogen-to-methane synthesis).

Schneider [21] found the efficiency of the conversion chain for the DBT-LOHC concept (4) to be 48% before the end-use, which is a lower efficiency than that for the pathway 2 (54%). With the advanced SOEC and the SOFC technology, the efficiency of the LOHC concept could increase to 86% before the end-use and to 43% over the whole conversion chain. This indicates energy losses of 22% for the LOHC concept between hydrogen production and end-use. Müller et al. [157] found better efficiency for the reversible storage than for the irreversible hydrogen storage in compensation of fluctuating power generation from renewable sources. The overall efficiency (electricity-to-electricity) based on reversible LOHCs was estimated to be appr. 30%. Irreversible hydrogen storage (hydrogen-to-liquid fuel) was considered as the best option for mobility.

Some evaluations of the integrated LOHC systems have indicated thermal efficiencies of over 60% and electricity generation efficiencies of appr. 40% [149,150,152,153]. In all cases the calculated efficiencies depend on the assumptions made.

Regarding the economical evaluations of hydrogen storages, assumptions may change over time as the prices are volatile and dependent on many factors, such as regional incentives and taxes. Also mandatory shifts to carbon-neutral energy are expected. The LOHC use in community heat and electricity has appeared to be reasonable at high residential electricity price (153.7 € per MWh). In this case, the LOHC system represented 11.6% of the electricity cost [158]. LOHC integrated in a wind park and a cement plant indicated reduction of annual costs by appr. 1 million €. The LOHC investment of 3.5 million € would be amortised in less than 10 years [151]. The overseas supply of hydrogen has pointed to lower costs for using LOHC than other options [16,23,60,146,147]. Also LOHC use in Indian conditions has been studied [159]. For decentralised hydrogen refuelling stations using

LOHC, costs for hydrogen have been estimated at around 6.5 € per kg in Japan [23,146,147]. A demonstration of logistics by charging DBT-LOHC with solar power in Erlangen and by road transport to Stuttgart to release hydrogen for EVs (30 kW) showed hydrogen delivery costs from 5 to 55 € per kg, while the market value of hydrogen at filling station would be 9–12 € per kg [42]. Preuster et al. [42] suggested that hydrogen as fuel for transport or industrial use is economically more attractive than conversion of hydrogen back into electricity.

An evaluation of costs, limited to conversion and transportation of hydrogen (hydrogen-to-user), gives an equal basis for comparison of different hydrogen storage options. Teichmann et al. [60] estimated costs for transportation of hydrogen in LOHC as 0.159 € per kg H₂ for 50 km distance and costs of hydrogenation and hydrogen release as 0.255 € per kg H₂ (in total 0.414 € per kg H₂). According to Yang and Odgen et al. [160], the costs of compression, liquefaction and storage of compressed and liquid hydrogen are in a range from \$0.1 to \$4 per kg H₂, and distribution costs to refuelling stations from \$1.1 to \$1.8 per kg H₂ (base case for 1800 kg per day stations). Differences were found in the preferences on gaseous or liquid hydrogen depending on transportation distances and hydrogen demand. For short distances and low hydrogen demand, transportation of compressed hydrogen with gas trucks was more economical than that of liquid hydrogen with trucks. The latter was economical for longer distances and larger demand, while pipelines were the most economical for the largest hydrogen demand. Reddi et al. [161] estimated that the costs for using tube trailer only for the delivery of compressed hydrogen varies from appr. \$1.5 to \$3 per kg H₂ (250–750 kg H₂ per day, 100–300 miles). Pipeline transportation of hydrogen is estimated to cost some \$1 per kg hydrogen [112].

Transportation costs for liquid fuels are very low, for example appr. \$0.01 per kg in the case of ethanol [162], and estimated in the same range for circular methanol. However, conversion of hydrogen to circular fuels is expensive. According to Hannula [126], production costs of methanol as electrofuel are appr. 40 € per GJ, and thus appr. 26 € per GJ without the costs of hydrogen. This means costs of 0.52 € per kg methanol and 3.1 € per kg H₂ (as energy equivalent).

5.9. Sufficiency of materials

Global energy needs are huge. For example, world energy supply was 13 550 Mtoe in 2013 [116] and only marine fuels are consumed appr. 350 Mt annually [163]. To cover 10% of the global energy supply, hydrogen demand would be 410 Mt, which is almost seven times more than the amount of hydrogen produced in 2013. To cover this hydrogen demand, 7500 Mt of material would be needed at the hydrogen storage capacity of 5.5 wt-%. These materials should consist of abundant elements, for example those in the Earth's crust (O, Si, Al, Na, H, K, Ca, Fe, Mg, Ti, C, F, P, Mg and S [164]). The rarest are the Pt group elements and Au, Rh, and Te.

The advantage of reversible hydrogen carriers is that the structure of material remains over hydrogenation and dehydrogenation cycles. Therefore, only a fraction of material is needed to carry the same

Table 3

Selected LOHC candidates and some examples of reaction conditions for their hydrogenation and dehydrogenation.

Dehydroge-nated form	Hydrogenation	Ref.	Dehydrogenation of hydrogenated form	Ref.	Dehydr. mp/bp; Hydr. mp/bp (°C)
Toluene	Ni cat, 95–125 °C, 20–40 atm	[27]	Pt/AC, Pd/AC > 300 °C	[38]	–95/111; –127/101
Xylenes	Cp*ZrBz2/ZrS, 25 °C, 7 atm, 1 h	[33]			< -25, < 13/139–144; < -37/120–125
Arenes	Various cat, 155–180 °C, 10–30 bar	[11]	Ir “pincer”, ~190 °C	[43]	Various compounds
Naphthalene (a3)	Ni cat, 80–160 °C, 20–40 bar	[29]	Pt-Rh/AC, 280 °C, 1 h “superheated liquid-film”	[39]	80/218; –43/187–196
DBT (a8)	Ru/Al ₂ O ₃ , 150 °C, 50 bar, 1 h	[24]	Pt/C, 290 °C, 210 min (faster at 310 °C)	[24]	–39/390; –58/-
NEC (b3)	Ru/Al ₂ O ₃ , 170 °C, 70 bar, 1 h	[65]	Pd/Al ₂ O ₃ , 180–220 °C, 4 h	[21,65]	69/378; 43/281
Quinaldine, quinoline	THQ < 200 °C, 10–70 bar; DHQ 175–260 °C, 110–210 bar, solvents	[87]	Ni-NiCrO, 350 °C, 5 h, benzene solvent	[78]	–15/237; –40/200
BuP (d5)			Ir PCP “pincer”, 140 °C, 18 h	[17]	–16/170; –13/154
NEI (d15)	Ru/Al ₂ O ₃ , 160–190 °C, 90 bar, 1.3 h, hexane solvent	[17,101]	Pd/Al ₂ O ₃ , 190 °C, 4 h	[17,101]	–18/253; 15/201

Table 4Pros and cons for compressed and liquid hydrogen, circular methanol and DBT-LOHC as hydrogen storages. Plus sign (+) means strength and a minus sign (–) a weakness. ^a

	CH ₂ (700 bar)	LH ₂ (–253 °C)	Circular methanol	DBT-LOHC
Energy density	– Appr. 5.0 MJ L ^{–1}	+ Appr. 8.5 MJ L ^{–1}	+ + Appr. 15.9 MJ L ^{–1}	+ Appr. 7.4 MJ kg ^{–1}
Reversibility	Not relevant	Not relevant	– – No	+ + Good
Maturity of technologies	+ Existing	+ Existing	+ + Good	+ Existing
Infrastructure compatibility	– – No	– – No	+ + + Excellent	+ + + Excellent
Transportation configuration	– Special (gas truck up to 1000 kg H ₂)	– Special (tube trailer, tanker 4000 kg H ₂)	+ + + Ordinary truck (equiv. 4000 kg H ₂)	+ + + Ordinary truck (1800 kg H ₂)
Transportation size, distance	– Limited (short distances, low demand)	– Limited (long distances, high demand)	+ + + Unlimited	+ + + Unlimited
Storage time (stability)	– Limited	– – Losses	+ + + Unlimited	+ + + Unlimited
Safety	– Concerns	– Concerns	± As gasoline	+ + + Excellent
Biodegradability	Not relevant	Not relevant	+ + + Excellent	– – Poor
Operability in dynamic use	+ Feasible	+ Feasible	+ + + Excellent	± Limited today
Efficiency loss in conversion and transportation	± Appr. 6–15%	– – Appr. 30% plus boil-off	– Appr. 19%	– Appr. 22%
Costs of transportation	– – Transportation \$0.1–4 ^b & distribution \$1.1–1.8 ^c per kg H ₂	– – Transportation \$0.1–4 ^b & distribution \$1.1–1.8 ^c per kg H ₂	– – – 3.1 € per kg H ₂ (energy equiv. hydrogen ^e)	– 0.4 € per kg H ₂ ^d (limited information)

^a References in Sections 5.1–5.9.^b Compression, liquefaction, storage, transportation.^c To refuelling stations without costs of stations.^d Hydrogenation, dehydrogenation, transportation.^e Production (conversion of hydrogen to methanol).

amount of energy as bound in the fossil fuels or in circular hydrogen carriers. However, even for some reversible hydrogen carriers sufficiency of materials is not evident in large-scale use. For example, replacing 10% of the global energy supply with hydrogen stored in ammonia borane would require 730 Mt of boron, while its global reserves are 110 Mt [165].

LOHCs based on aromatics would be scalable as they contain only carbon and hydrogen. Global volume of aromatic building blocks (benzene and toluene) is more than 50 Mt annually at a price below 1 € per kg. Crude oil contains aromatics, and they are produced by catalytic reforming in oil refineries. Renewable aromatics could be processed from lignin. Production of dibenzyltoluenes could easily grow. The global production of heat transfer fluids was only 466 kt in 2014 and only partly based on DBT [166]. <http://www.grandviewresearch.com/industry-analysis/heat-transfer-fluids-market> Nitrogen containing aromatics, such as NEC, can be produced from crude oil, coal or lignin. Production of NEC is limited today and ethylation of carbazole generates a large amount of wastes (e.g. KCl or K₂SO₄) [167].

The sufficiency of catalysts also deserves consideration, although they are largely recyclable. If the dehydrogenation of 500 tonnes of LOHC required one kilogram of catalyst at a price of 150 € per kg [61,168], dehydrogenation of 7500 Mt of LOHC would need 15 kt of catalyst. This is only a fraction of the world resources of Pt group metals as over 100 kt of these can be economically mined [169]. However, annual production of Pt was only 0.183 kt in 2012 [170]. Reversible

hydrogen carriers would reduce the global consumption of catalysts and other materials for energy purposes. However, all manufacturing should be based on efficient and green processes, and thus developing metal-free catalysts for the LOHC cycle is a sustainable approach.

Circular hydrogen carriers are in principle abundant when produced from renewable hydrogen and CO₂ or nitrogen. Extraction of CO₂ from air is neither a mature nor economical technology today, while extracting CO₂ from industrial flue gas more feasible. However, suitable flue gas may be located in a different region than the best renewable hydrogen sources. Ammonia production based on atmospheric nitrogen is an energy-consuming process. Furthermore, circular hydrogen carriers are not reversible as new batches are needed for each cycle.

6. Conclusions

The large-scale development of renewable energy is dependent on hydrogen, as other means for storing solar and wind energy have their limitations. For example, the storage times of batteries are short, while pumped hydro and compressed air regimes are inflexible and unsuitable for all locations. The main challenges limiting hydrogen implementation are related to its production and storage. Many hydrogen storage options have been proposed with the feasibility of different strategies dependent on the demands of their target sectors. For example, in the transport sector and residential use, the energy density, hydrogen release rate and safety are of primary importance, while

different criteria apply when hydrogen is used as a seasonal storage or to buffer power fluctuations.

Table 4 summarises the relative strengths and weaknesses of compressed and liquid hydrogen, circular methanol and the LOHC concept. Solid materials that can adsorb and desorb hydrogen are not included as the technologies are immature and cannot be integrated with the existing infrastructure.

Compressed and liquid hydrogen can be economical and feasible solutions for appropriate transport distances and hydrogen volumes. However, compressed hydrogen has a low energy density while the energy density of liquid hydrogen is substantially reduced by liquefaction and boil-off losses. Furthermore, the scale-up of these options is limited by infrastructure needs. Given the prevalence of fossil fuels, circular energy carriers such as methanol and hydrocarbons are attractive options as they can be seamlessly integrated with current technologies. This is an important aspect for sectors most reliant on liquid fuels, such as aviation and shipping. However, production costs of circular fuels are high and continuous production is required. Furthermore, wind and solar energy is often located far from feasible carbon dioxide sources and the technology for extracting atmospheric CO₂ is not yet economical. Ammonia-based circular fuels also suffer from the safety concerns.

LOHCs can be reversibly hydrogenated and dehydrogenated using catalysts at elevated temperatures. LOHCs act as “liquid hydrogen batteries” as their structures converge over the hydrogenation/dehydrogenation cycle. Dibenzyl toluenes and toluene LOHC concepts are already commercial in Germany and Japan. These LOHCs have many good features: reasonable gravimetric and volumetric hydrogen storage densities, extensive ranges of storage times and capacities, a liquid state at normal temperature and pressure and compatibility with the infrastructure for liquid fuels. DBT-LOHCs are also safe liquids to handle and use. The total efficiency of the DBT-LOHC pathway with waste heat utilisation is comparable to other hydrogen based pathways. Challenges with LOHC systems are related to the limited experience with this relatively new technology. For example, system durability, hydrogen release rate and catalyst performance in long-term use needs to be proven. Further development towards hydrogen release at mild reaction conditions would improve the energy balance of the LOHC system.

An energy revolution viz. continuous growth of renewable energy requires solutions for its transportation and storage in a large-scale and for the long-term, and also for demanding use. Different hydrogen storage options have been proposed and it is not likely that one solution will be optimal for all purposes. Hydrogen storage technologies are developing with costs decreasing on scaled production. LOHCs and circular hydrogen carriers (for example methanol and hydrocarbons) are attractive, safe and flexible options that could offer feasible solutions to fill in the gaps in the storage sizes and times for renewable energy. Techno-economical evaluations of the best uses of different hydrogen carriers are needed to create an understanding of the pathways towards their successful integration in the energy infrastructure. In the face of the energy revolution, hydrogen storage solutions are needed to support the transition to low carbon energy.

Acknowledgements

The authors acknowledge financial support for the LOHCNESS project (<http://www.vtt.fi/sites/lohcnness>) from Tekes (1508/31/2017), and from industrial partners, Fortum, St1 Renewable Energy Oy, Oy Woikoski Ab, Leppäkosken Sähkö Oy and Aino Energia Oy. Acknowledgements are given to Jari Ihonen at VTT for informative discussions, and to reviewers for valuable comments and remarks.

Appendix A. Supplementary data

Supplementary data related to this article can be found at <https://doi.org/10.1016/j.jpowsour.2018.04.011>.

References

- [1] IEA, Key Renewables Trends, Excerpt from: Renewables Information, (2015), p. 8, <https://doi.org/10.1787/renew-2015-en>.
- [2] IEA, Renewable Energy Outlook, (2013) http://www.worldenergyoutlook.org/media/weowebsite/2013/WEO2013_Ch06_Renewables.pdf%5Cnhttp://www.worldenergyoutlook.org/publications/weo-2013/.
- [3] M. Ball, M. Wietschel, The Hydrogen Economy: Opportunities and Challenges, Cambridge University Press, Cambridge, 2009.
- [4] T. Randall, Fossil Fuels Just Lost the Race against Renewables, (2015).
- [5] IEA, Technology Roadmap: Hydrogen and Fuel Cells, (2015), https://doi.org/10.1007/SpringerReference_7300.
- [6] T. Lipman, An Overview of Hydrogen Production and Storage Systems with Renewable Hydrogen Case Studies, Clean Energy States Alliance, 2011, p. 32, <https://doi.org/10.1017/CBO9781107415324.004>.
- [7] R.H. Crabtree, Hydrogen storage in liquid organic heterocycles, Energy Environ. Sci. (2008) 134–138, <https://doi.org/10.1039/b805644g>.
- [8] H. Turunen, CO₂-balance in the Atmosphere and CO₂-utilisation: an Engineering Approach, University of Oulu, Academic d, 2011.
- [9] M. Markiewicz, Y.Q. Zhang, A. Bösmann, N. Brückner, J. Thöming, P. Wasserscheid, S. Stolte, Environmental and health impact assessment of Liquid Organic Hydrogen Carrier (LOHC) systems – challenges and preliminary results, Energy Environ. Sci. 8 (2015) 1035–1045, <https://doi.org/10.1039/C4EE03528C>.
- [10] A. Moores, M. Poyatos, Y. Luo, R.H. Crabtree, Catalysed low temperature H₂ release from nitrogen heterocycles, New J. Chem. 30 (2006) 1675, <https://doi.org/10.1039/b608914c>.
- [11] C. Bianchini, A. Meli, F. Vizza, Hydrogenation of arenes and heteroatoms, in: J.G. de Vries, C.J. Elsevier (Eds.), Handbook of Homogeneous Hydrogenation, vol. 2, Wiley-VCH, Weinheim, Germany, 2007.
- [12] F. Sotoodeh, B.J.M. Huber, K.J. Smith, The effect of the N atom on the dehydrogenation of heterocycles used for hydrogen storage, Appl. Catal. Gen. 419–420 (2012) 67–72, <https://doi.org/10.1016/j.apcata.2012.01.013>.
- [13] D. Dean, P.G. Jessop, The effect of temperature, catalyst and sterics on the rate of N -heterocycle dehydrogenation for hydrogen storage, New J. Chem. (2011) 417–422, <https://doi.org/10.1039/c0nj00511h>.
- [14] J. Von Wild, T. Friedrich, A. Cooper, B. Toseland, G. Muraro, W. Tegrotenhuis, Y. Wang, P. Humble, A. Karim, Liquid Organic Hydrogen Carriers (LOHC): an auspicious alternative to conventional hydrogen storage technologies, 18th World Hydrog. Energy Conf vol. 78, (2010), pp. 189–197.
- [15] A.C. Cooper, K.M. Campbell, G.P. Pez, An integrated hydrogen storage and delivery approach using organic liquid-phase carriers, 16th World Hydrog. Energy Conf. 2006, pp. 1–12.
- [16] A. Bourane, M. Elanany, T. V. Pham, S.P. Katikaneni, An overview of organic liquid phase hydrogen carriers, Int. J. Hydrogen Energy 41 (2016) 23075–23091, <https://doi.org/10.1016/j.ijhydene.2016.07.167>.
- [17] C. Jensen, D. Brayton, S. Jorgensen, Development of a Practical Hydrogen Storage System Based on Liquid Organic Hydrogen Carriers and a Homogeneous Catalyst (IV.E.2) vol. 1, (2013), pp. 135–139.
- [18] T. He, Q. Pei, P. Chen, Liquid organic hydrogen carriers, J. Energy Chem. 24 (2015) 587–594, <https://doi.org/10.1016/j.jechem.2015.08.007>.
- [19] K. Müller, K. Stark, B. Müller, W. Arlt, Amine borane based hydrogen carriers: an evaluation, Energy Fuels 26 (2012) 3691–3696, <https://doi.org/10.1021/ef300516m>.
- [20] R.H. Crabtree, Nitrogen-containing liquid organic hydrogen carriers: progress and prospects, Sustain. Chem (2017) 4491–4498, <https://doi.org/10.1021/acssuschemeng.7b00983>.
- [21] M.J. Schneider, Hydrogen Storage and Distribution via Liquid Organic Carriers, (2015).
- [22] D. Geburtig, P. Preuster, A. Bösmann, K. Müller, P. Wasserscheid, Chemical utilization of hydrogen from fluctuating energy sources - catalytic transfer hydrogenation from charged Liquid Organic Hydrogen Carrier systems, Int. J. Hydrogen Energy 41 (2016) 1010–1017, <https://doi.org/10.1016/j.ijhydene.2015.10.013>.
- [23] Y. Okada, E. Sasaki, E. Watanabe, S. Hyodo, H. Nishijima, Development of dehydrogenation catalyst for hydrogen generation in organic chemical hydride method, Int. J. Hydrogen Energy 31 (2006) 1348–1356, <https://doi.org/10.1016/j.ijhydene.2005.11.014>.
- [24] N. Brückner, K. Obesser, A. Bösmann, D. Teichmann, W. Arlt, J. Dungs, P. Wasserscheid, Evaluation of industrially applied heat-transfer fluids as liquid organic hydrogen Carrier systems, ChemSusChem. 7 (2014) 229–235, <https://doi.org/10.1002/cssc.201300426>.
- [25] O. Sultan, H. Shaw, Study of automotive storage of hydrogen using recyclable liquid chemical carriers, Energy Prod. Convers (1975) 589.
- [26] M. Taube, D.W. Rippin, D.L. Cresswell, W. Knecht, A system of hydrogen-powered vehicles with liquid organic hydrides, Int. J. Hydrogen Energy 8 (1983) 213–225.
- [27] S. Toppinen, T.-K. Rantakylä, T. Salmi, J. Aittamaa, Kinetics of the liquid-phase hydrogenation of benzene and some monosubstituted alkylbenzenes, Ind. Eng. Chem. Res. 35 (1996) 1824–1833, <https://doi.org/10.1021/ie9504314>.
- [28] V.L. Barrio, P.L. Arias, J.F. Cambra, M.B. Güemez, B. Pawelec, J.L.G. Fierro, Aromatics Hydrogenation on Silica – Alumina Supported Palladium – Nickel Catalysts vol. 242, (2003), pp. 17–30.
- [29] P. Rautanen, M. Lylykangas, J. Aittamaa, O. Krause, Liquid-phase hydrogenation of naphthalene and tetralin on Ni/Al₂O₃: kinetic modeling, Ind. Eng. Chem. Res. 41 (2002) 5966–5975, <https://doi.org/10.1021/ie020395q>.
- [30] S.R. Kirumakki, B.G. Shpeizer, V.G. Sagar, K.V.R. Chary, A. Clearfield,

- Hydrogenation of naphthalene over NiO/SiO₂-Al₂O₃ catalysts: structure–activity correlation, *J. Catal.* 242 (2006) 319–331, <https://doi.org/10.1016/j.jcat.2006.06.014>.
- [31] K. Sakanishi, M. Ohira, I. Mochida, H. Okazaki, M. Soeda, The reactivities of polyaromatic hydrocarbons in catalytic hydrogenation over supported noble metals, *Bull. Chem. Soc. Jpn.* 62 (1989) 3994–4001.
- [32] B. Sun, F.-A. Khan, A. Vallat, G. Süß-Fink, NanoRu@hectorite: a heterogeneous catalyst with switchable selectivity for the hydrogenation of quinoline, *Appl. Catal. Gen.* 467 (2013) 310–314, <https://doi.org/10.1016/j.apcata.2013.07.037>.
- [33] M.M. Stalzer, C.P. Nicholas, A. Bhattacharyya, A. Motta, M. Delferro, T.J. Marks, Single-face/all- Cis Arene Hydrogenation by a Supported Single-site D 0 Organozirconium Catalyst *Angewandte*, (2016), pp. 5263–5267, <https://doi.org/10.1002/anie.201600345>.
- [34] S.J. Geier, P.A. Chase, D.W. Stephan, Metal-free reductions of N-heterocycles via Lewis acid catalyzed hydrogenation, *Chem. Commun.* 46 (2010) 4884–4886, <https://doi.org/10.1039/c0cc00719f>.
- [35] K. Chernichenko, A. Madarász, I. Pápai, M. Nieger, M. Leskelä, T. Repo, A frustrated-Lewis-pair approach to catalytic reduction of alkynes to cis-alkenes, *Nat. Chem.* 5 (2013) 718–723, <https://doi.org/10.1038/nchem.1693>.
- [36] D. Sebastián, E.G. Bordejé, L. Calvillo, M.J. Lázaro, R. Moliner, Hydrogen storage by decalin dehydrogenation/naphthalene hydrogenation pair over platinum catalysts supported on activated carbon, *Int. J. Hydrogen Energy* 33 (2008) 1329–1334, <https://doi.org/10.1016/j.ijhydene.2007.12.037>.
- [37] K. Owen, T. Coley, *Automotive Fuels Reference Book*, second ed., Society of Automotive Engineers, Warrendale, 1995.
- [38] N. Kariya, A. Fukuoka, M. Ichikawa, Efficient evolution of hydrogen from liquid cycloalkanes over Pt-containing catalysts supported on active carbons under “wet – dry multiphase conditions”, *Appl. Catal.* 233 (2002) 91–102.
- [39] S. Hodoshima, S. Takaiwa, A. Shono, K. Satoh, Y. Saito, Hydrogen Storage by Decalin/naphthalene Pair and Hydrogen Supply to Fuel Cells by Use of Superheated Liquid-film-type Catalysts vol. 283, (2005), pp. 235–242, <https://doi.org/10.1016/j.apcata.2005.01.010>.
- [40] M. Taube, P. Taube, A Liquid Organic Carrier of Hydrogen as a Fuel for Automobiles (Nuclear Power as a Motive Power for Cars), (1979).
- [41] A. Shukla, S. Karmakar, R.B. Biniwale, Hydrogen delivery through liquid organic hydrides: considerations for a potential technology, *Int. J. Hydrogen Energy* 37 (2011) 3719–3726, <https://doi.org/10.1016/j.ijhydene.2011.04.107>.
- [42] P. Preuster, C. Papp, P. Wasserscheid, Liquid organic hydrogen carriers (LOHCs): toward a hydrogen-free hydrogen economy, *Acc. Chem. Res.* 50 (2017) 74–85, <https://doi.org/10.1021/acs.accounts.6b00474>.
- [43] C.M. Jensen, U. S. Patent 6,074,447, 2000.
- [44] Z. Wang, I. Tonks, J. Belli, C.M. Jensen, Dehydrogenation of N-ethyl perhydrocarbazole catalyzed by PCP pincer iridium complexes: evaluation of a homogeneous hydrogen storage system, *J. Organomet. Chem.* 694 (2009) 2854–2857, <https://doi.org/10.1016/j.jorgchem.2009.03.052>.
- [45] K. Müller, K. Stark, V.N. Emelyanenko, M.A. Varfolomeev, D.H. Zaitsau, E. Shoifet, C. Schick, S.P. Verevkin, W. Arlt, Liquid organic hydrogen carriers: thermo-physical and thermochemical studies of benzyl- and dibenzyl-toluene derivatives, *Ind. Eng. Chem. Res.* 54 (2015) 7967–7976, <https://doi.org/10.1021/acs.iecr.5b01840>.
- [46] Anon, EC-safety DATA SHEET: MARLOHC 18/90, (2017), pp. 1–11.
- [47] Anon., Marlotherm® SH product information, (n.d.).
- [48] G. Do, P. Preuster, R. Aslam, A. Bosmann, K. Müller, W. Arlt, P. Wasserscheid, Hydrogenation of the liquid organic hydrogen Carrier compound dibenzyltoluene - reaction pathway determination by 1H NMR spectroscopy, *R. Soc. Chem.* 1 (2016) 313–320, <https://doi.org/10.1039/C5RE00080G>.
- [49] R. Aslam, M. Minceva, K. Müller, W. Arlt, Development of a liquid chromatographic method for the separation of a liquid organic hydrogen Carrier mixture, *Separ. Purif. Technol.* 163 (2016) 140–144, <https://doi.org/10.1016/j.seppur.2016.01.051>.
- [50] K. Müller, R. Aslam, A. Fischer, K. Stark, P. Wasserscheid, W. Arlt, Experimental Assessment of the Degree of Hydrogen Loading for the Dibenzyl Toluene Based LOHC System vol. 1, (2016), pp. 2–8, <https://doi.org/10.1016/j.ijhydene.2016.09.196>.
- [51] P. Inhetveen, N.S.A. Alt, E. Schluecker, Measurement of the hydrogenation level of dibenzyltoluene in an innovative energy storage system, *Vib. Spectrosc.* 83 (2016) 85–93, <https://doi.org/10.1016/j.vibspec.2016.01.008>.
- [52] R. Aslam, K. Müller, M. Müller, M. Koch, P. Wasserscheid, W. Arlt, Measurement of hydrogen solubility in potential liquid organic hydrogen carriers, *J. Chem. Eng. Data* 61 (2016) 643–649, <https://doi.org/10.1021/acs.jced.5b00789>.
- [53] A. Heller, M.H. Rausch, P.S. Schulz, P. Wasserscheid, A.P. Fröba, Binary diffusion coefficients of the liquid organic hydrogen Carrier system dibenzyltoluene/perhydrodibenzyltoluene, *J. Chem. Eng. Data* 61 (2016) 504–511, <https://doi.org/10.1021/acs.jced.5b00671>.
- [54] H. Jorschick, P. Preuster, S. Dürr, A. Seidel, K. Müller, A. Bösmann, P. Wasserscheid, Hydrogen storage using a hot pressure swing reactor, *Energy Environ. Sci.* (2017), <https://doi.org/10.1039/C7EE00476A>.
- [55] M. Amende, A. Kaftan, P. Bachmann, R. Brehmer, P. Preuster, M. Koch, P. Wasserscheid, J. Libuda, Regeneration of LOHC dehydrogenation catalysts: in-situ IR spectroscopy on single crystals, model catalysts, and real catalysts from UHV to near ambient pressure, *Appl. Surf. Sci.* 360 (2016) 671–683, <https://doi.org/10.1016/j.apsusc.2015.11.045>.
- [56] A. Fikrt, R. Brehmer, V. Milella, K. Müller, A. Bösmann, P. Preuster, N. Alt, E. Schlücker, P. Wasserscheid, W. Arlt, Dynamic power supply by hydrogen bound to a liquid organic hydrogen Carrier, *Appl. Energy* 194 (2017) 1–8, <https://doi.org/10.1016/j.apenergy.2017.02.070>.
- [57] P. Frentzos, D. McKinney, Dibenzyltoluene and partially hydrogenated terphenyls. A review of the distinguishing molecular and physical properties of Dibenzyltoluene and Partially Hydrogenated Terphenyls in heat transfer applications., (n.d.).
- [58] J.S. Sung, K.Y. Choo, T.H. Kim, A.L. Tarasov, O.P. Tkachenko, L.M. Kustov, A new hydrogen storage system based on efficient reversible catalytic hydrogenation/dehydrogenation of terphenyl, *Int. J. Hydrogen Energy* 33 (2008) 2721–2728, <https://doi.org/10.1016/j.ijhydene.2008.03.037>.
- [59] D. Teichmann, W. Arlt, P. Wasserscheid, R. Freymann, A future energy supply based on Liquid Organic Hydrogen Carriers (LOHC), *Energy Environ. Sci.* 4 (2011) 2767–2773, <https://doi.org/10.1039/c1ee01454d>.
- [60] D. Teichmann, W. Arlt, P. Wasserscheid, Liquid Organic Hydrogen Carriers as an efficient vector for the transport and storage of renewable energy, *Int. J. Hydrogen Energy* 37 (2012) 18118–18132, <https://doi.org/10.1016/j.ijhydene.2012.08.066>.
- [61] D. Teichmann, K. Stark, K. Müller, G. Zöttl, P. Wasserscheid, W. Arlt, Energy storage in residential and commercial buildings via Liquid Organic, *Energy Environ. Sci.* 5 (2012) 9044–9054, <https://doi.org/10.1039/c2ee22070a>.
- [62] Z. Jiang, Q. Pan, J. Xu, T. Fang, Current situation and prospect of hydrogen storage technology with new organic liquid, *Int. J. Hydrogen Energy* 39 (2015) 17442–17451, <https://doi.org/10.1016/j.ijhydene.2014.01.199>.
- [63] A.F. Dalebrook, W. Gan, M. Grasemann, Hydrogen storage: beyond conventional methods, *ChemComm* 49 (2013) 8735–8751, <https://doi.org/10.1039/c3cc43836h>.
- [64] G. Pez, A. Scott, A. Cooper, H. Cheng, L. Bagzis, J. Appleby, Hydrogen Storage Reversible Hydrogenated of Pi-conjugated Substrates, *WO 2005/000457* (2005).
- [65] M. Yang, Y. Dong, S. Fei, H. Ke, H. Cheng, A comparative study of catalytic dehydrogenation of perhydro-N-ethylcarbazole over noble metal catalysts, *Int. J. Hydrogen Energy* 39 (2014) 18976–18983, <https://doi.org/10.1016/j.ijhydene.2014.09.123>.
- [66] C. Gleichweit, M. Amende, U. Bauer, S. Schernich, O. Höfert, M.P.A. Lorenz, W. Zhao, M. Müller, M. Koch, P. Bachmann, P. Wasserscheid, J. Libuda, H. Steinrück, C. Gleichweit, M. Amende, U. Bauer, S. Schernich, O. Höfert, P. Wasserscheid, J. Libuda, H. Steinrück, C. Papp, Alkyl Chain Length-dependent Surface Reaction of Dodecahydro-N-alkylcarbazoles on Pt Model Catalysts Alkyl Chain Length-dependent Surface Reaction of Dodecahydro-N-alkylcarbazoles on Pt Model Catalysts vol. 54701, (2014), pp. 0–9, <https://doi.org/10.1063/1.4875921>.
- [67] K. Stark, P. Keil, S. Schug, K. Mu, P. Wasserscheid, W. Arlt, Melting points of potential liquid organic hydrogen Carrier systems Consisting of N-alkylcarbazoles, *J. Chem. Data* 61 (2016) 1441–1448, <https://doi.org/10.1021/acs.jced.5b00679>.
- [68] F. Sotoodeh, L. Zhao, K.J. Smith, Kinetics of H₂ recovery from dodecahydro-N-ethylcarbazole over a supported Pd catalyst, *Appl. Catal. Gen.* 362 (2009) 155–162, <https://doi.org/10.1016/j.apcata.2009.04.039>.
- [69] M. Yang, Y. Dong, H. Cheng, Hydrogenation Kinetics of N-ethylcarbazole as a heteroaromatic liquid organic hydrogen carrier, *Adv. Mater. Res.* 953–954 (2014) 981–984.
- [70] K.M. Eblagon, D. Rentsch, O. Friedrichs, A. Remhof, A. Zuetzel, A.J. Ramirez-Cuesta, S.C. Tsang, Hydrogenation of 9-ethylcarbazole as a prototype of a liquid hydrogen Carrier, *Int. J. Hydrogen Energy* 35 (2010) 11609–11621, <https://doi.org/10.1016/j.ijhydene.2010.03.068>.
- [71] M. Amende, S. Schernich, M. Sobota, I. Nikiforidis, H. Drescher, C. Papp, H. Steinrück, A. Göring, P. Wasserscheid, M. Laurin, J. Libuda, Dehydrogenation mechanism of liquid organic hydrogen carriers: dodecahydro-N-ethylcarbazole on Pd(111), *Chem. Eur. J.* 19 (2013) 10854–10865, <https://doi.org/10.1002/chem.201301323>.
- [72] X. Ye, Y. An, G. Xu, Kinetics of 9-ethylcarbazole hydrogenation over Raney-Ni catalyst for hydrogen storage, *J. Alloy. Comp.* 509 (2011) 152–156, <https://doi.org/10.1016/j.jallcom.2010.09.012>.
- [73] K.M. Eblagon, K. Tam, S.C.E. Tsang, Comparison of catalytic performance of supported ruthenium and rhodium for hydrogenation of 9-ethylcarbazole for hydrogen storage applications, *Energy Environ. Sci.* 5 (2012) 8621–8630, <https://doi.org/10.1039/c2ee22066k>.
- [74] A. Mehranfar, M. Izadyar, A.A. Esmaeili, Hydrogen storage by N-ethylcarbazole as a new liquid organic hydrogen Carrier: a DFT study on the mechanism, *Int. J. Hydrogen Energy* 40 (2015) 5797–5806, <https://doi.org/10.1016/j.ijhydene.2015.03.011>.
- [75] C. Wan, Y. An, G. Xu, W. Kong, Study of catalytic hydrogenation of N-ethylcarbazole over ruthenium catalyst, *Int. J. Hydrogen Energy* 37 (2012) 13092–13096, <https://doi.org/10.1016/j.ijhydene.2012.04.123>.
- [76] D. Forberg, T. Schwob, M. Zaheer, M. Friedrich, N. Miyajima, R. Kempe, Single-catalyst high-weight% hydrogen storage in an N-heterocycle synthesized from lignin hydrogenolysis products and ammonia, *Nat. Commun.* 7 (2016) 13201, <https://doi.org/10.1038/ncomms13201>.
- [77] W. Peters, M. Eypasch, T. Frank, J. Schwerdtfeger, C. Körner, A. Bösmann, P. Wasserscheid, Efficient hydrogen release from perhydro-N-ethylcarbazole using catalyst-coated metallic structures produced by selective electron beam melting, *Energy Environ. Sci.* 8 (2015) 641–649, <https://doi.org/10.1039/C4EE03461A>.
- [78] H. Adkins, L.G. Lundsted, Catalytic dehydrogenation of hydroaromatic compounds in benzene. V. Application to pyrrolidines and piperidines, *J. Am. Chem. Soc.* 71 (1949) 2964–2965.
- [79] J. Yang, A. Sudik, C. Wolverton, D.J. Siegel, High capacity hydrogen storage materials: attributes for automotive applications and techniques for materials discovery, *Chem. Soc. Rev.* (2010) 656–675, <https://doi.org/10.1039/b802882f>.
- [80] F. Sotoodeh, B.J.M. Huber, K.J. Smith, Dehydrogenation kinetics and catalysis of

- organic heteroaromatics for hydrogen storage, *Int. J. Hydrogen Energy* 37 (2012) 2715–2722, <https://doi.org/10.1016/j.ijhydene.2011.03.055>.
- [81] M. Yang, C. Han, G. Ni, J. Wu, H. Cheng, Temperature controlled three-stage catalytic dehydrogenation and cycle performance of perhydro-9-ethylcarbazole, *Int. J. Hydrogen Energy* 37 (2012) 12839–12845, <https://doi.org/10.1016/j.ijhydene.2012.05.092>.
- [82] M. Yang, Y. Dong, S. Fei, Q. Pan, G. Ni, C. Han, H. Ke, Q. Fang, H. Cheng, Hydrogenation of N-propylcarbazole over supported ruthenium as a new prototype of liquid organic hydrogen carriers (LOHC), *RSC Adv.* 3 (2013) 24877–24881, <https://doi.org/10.1039/c3ra44760j>.
- [83] I.Y. Choi, B.S. Shin, S.K. Kwak, K.S. Kang, C.W. Yoon, J.W. Kang, Thermodynamic efficiencies of hydrogen storage processes using carbazole-based compounds, *Int. J. Hydrogen Energy* 41 (2016) 9367–9373, <https://doi.org/10.1016/j.ijhydene.2016.04.118>.
- [84] O.Y. Gutiérrez, A. Hrabar, J. Hein, Y. Yu, J. Han, J.A. Lercher, Ring opening of 1,2,3,4-tetrahydroquinoline and decahydroquinoline on MoS₂/c-Al₂O₃ and Ni-MoS₂/c-Al₂O₃, *J. Catal.* 295 (2012) 155–168, <https://doi.org/10.1016/j.jcat.2012.08.003>.
- [85] J. Zhao, H. Chen, J. Xu, J. Shen, Effect of surface acidic and basic properties of the supported nickel catalysts on the hydrogenation of pyridine to piperidine, *J. Phys. Chem. C* 15 (2013) 10573–10580, <https://doi.org/10.1021/jp402238q>.
- [86] J. Oh, K. Jeong, T.W. Kim, H. Kwon, J.W. Han, J.H. Park, Y.-W. Suh, A potential liquid organic hydrogen Carrier: 2-(n-methylbenzyl) pyridine with fast H₂ release and stable activity in consecutive hydrogenation-dehydrogenation cycles, *ChemSusChem* (2018), <https://doi.org/10.1002/cssc.201702256>.
- [87] M. Campanati, A. Vaccari, O. Piccolo, Mild hydrogenation of quinoline. Role of reaction parameters, *J. Mol. Catal. Chem.* 179 (2002) 287–292, [https://doi.org/10.1016/S1381-1169\(01\)00401-0](https://doi.org/10.1016/S1381-1169(01)00401-0).
- [88] M. Campanati, M. Casagrande, I. Fagiolo, M. Lenarda, L. Storaro, M. Battagliarin, A. Vaccari, Mild hydrogenation of quinoline 2. A novel Rh-containing pillared layered clay catalyst, *J. Mol. Catal. Chem.* 184 (2002) 267–272, [https://doi.org/10.1016/S1381-1169\(02\)00003-1](https://doi.org/10.1016/S1381-1169(02)00003-1).
- [89] F. Chen, A.-E. Surkus, L. He, M.-M. Pohl, J. Radnik, C. Topf, K. Junge, M. Beller, Selective catalytic hydrogenation of heteroarenes with N-graphene-modified cobalt nanoparticles (Co₃O₄-Co/NGr@α-Al₂O₃), *J. Am. Chem. Soc.* 137 (2015) 11718–11724, <https://doi.org/10.1021/jacs.5b06496>.
- [90] G. Fan, J. Wu, Mild hydrogenation of quinoline to decahydroquinoline over rhodium nanoparticles entrapped in aluminum oxy-hydroxide, *Catcom* 31 (2013) 81–85, <https://doi.org/10.1016/j.catcom.2012.11.015>.
- [91] R.A. Sánchez-Delgado, N. Machalaba, N. Ng-a-qui, Hydrogenation of quinoline by ruthenium nanoparticles immobilized on poly(4-vinylpyridine), *Catal. Commun.* 8 (2007) 2115–2118, <https://doi.org/10.1016/j.catcom.2007.04.006>.
- [92] F. Fache, Solvent dependent regioselective hydrogenation of substituted quinolines, *Synlett* (2004) 2827–2829, <https://doi.org/10.1055/s-2004-835654>.
- [93] J. Wu, D. Talwar, S. Johnston, M. Yan, J. Xiao, Acceptorless dehydrogenation of nitrogen heterocycles with a versatile iridium catalyst, *Angew. Chem. Int. Ed.* 52 (2013) 6983–6987, <https://doi.org/10.1002/anie.201300292>.
- [94] M.G. Manas, L.S. Sharninghausen, E. Lin, R.H. Crabtree, Iridium catalyzed reversible dehydrogenation - hydrogenation of quinoline derivatives under mild conditions, *J. Organomet. Chem.* 792 (2015) 184–189, <https://doi.org/10.1016/j.jorganchem.2015.04.015>.
- [95] K.I. Fujita, Y. Tanaka, M. Kobayashi, R. Yamaguchi, Homogeneous perdehydrogenation and perhydrogenation of fused bicyclic N-heterocycles catalyzed by iridium complexes bearing a functional bipyridonate ligand, *J. Am. Chem. Soc.* 136 (2014) 4829–4832, <https://doi.org/10.1021/ja5001888>.
- [96] S. Chakraborty, W.W. Brennessel, W.D. Jones, A molecular iron catalyst for the acceptorless dehydrogenation and hydrogenation of N-heterocycles, *J. Am. Chem. Soc.* 136 (2014) 8564–8567, <https://doi.org/10.1021/ja504523b>.
- [97] D.W. Stephan, G. Erker, Frustrated Lewis pairs: metal-free hydrogen activation and more, *Angew. Chem. Int. Ed.* 49 (2010) 46–76, <https://doi.org/10.1002/anie.200903708>.
- [98] D. Zhu, H. Jiang, L. Zhang, X. Zheng, H. Fu, M. Yuan, H. Chen, R. Li, Aqueous phase hydrogenation of quinoline to decahydroquinoline catalyzed by ruthenium nanoparticles supported on glucose-derived carbon spheres, *ChemCatChem* (2014) 2954–2960, <https://doi.org/10.1002/cctc.201402519>.
- [99] A. Roucoux, K. Philippot, *Handbook of Homogeneous Hydrogenation* vol. 2, Wiley-VCH, Weinheim, Germany, 2007.
- [100] T. Hara, K. Mori, T. Mizugaki, K. Ebata, K. Kaneda, Highly Efficient Dehydrogenation of Indolines to Indoles Using Hydroxyapatite-bound Pd Catalyst vol. 44, (2003), pp. 6207–6210.
- [101] Y. Dong, M. Yang, Z. Yang, H. Ke, H. Cheng, Catalytic hydrogenation and dehydrogenation of N-ethylindole as a new heteroaromatic liquid organic hydrogen carrier, *Int. J. Hydrogen Energy* 40 (2015) 10918–10922, <https://doi.org/10.1016/j.ijhydene.2015.05.196>.
- [102] D.F. Brayton, C.M. Jensen, Dehydrogenation of pyrrolidine based liquid organic hydrogen carriers by an iridium pincer catalyst, an isothermal kinetic study, *Int. J. Hydrogen Energy* 40 (2015) 16266–16270, <https://doi.org/10.1016/j.ijhydene.2015.10.014>.
- [103] Y. Cui, S. Kwok, A. Bucholtz, B. Davis, R.A. Whitney, P.G. Jessop, The effect of substitution on the utility of piperidines and octahydroindoles for reversible hydrogen storage, *New J. Chem.* 32 (2008) 1027–1037, <https://doi.org/10.1039/B718209K>.
- [104] C.M. Araujo, D.L. Simone, S.J. Konezny, A. Shim, R.H. Crabtree, G.L. Soloveichik, V.S. Batista, Fuel selection for a regenerative organic fuel cell/flow battery: thermodynamic considerations, *Energy Environ. Sci.* 5 (2012) 9534–9542, <https://doi.org/10.1039/c2ee22749e>.
- [105] P.F. Driscoll, E. Deunf, L. Rubin, J. Arnold, J.B. Kerr, Electrochemical redox catalysis for electrochemical dehydrogenation of liquid hydrogen Carrier fuels for energy storage and conversion, *J. Electrochem. Soc.* 7 (2013) 3152–3158, <https://doi.org/10.1149/2.024307jes>.
- [106] J.M. Hanlon, *Synthesis and Characterisation of Direct and Indirect Hydrogen Storage Materials*, University of Glasgow, 2013.
- [107] D. Fan, L. Wang, J. Huo, H. Yu, Recent Research Progress in Developing Metal Doped Porous Matrices for Hydrogen Storage vol. 61, (2018), pp. 2025–2035.
- [108] D. Pukazhavelan, V. Kumar, S.K. Singh, High capacity hydrogen storage: basic aspects, new developments and milestones, *Nanomater. Energy* 1 (2012) 566–589, <https://doi.org/10.1016/j.nanoen.2012.05.004>.
- [109] Y. Song, New perspectives on potential hydrogen storage materials using high pressure, *Phys. Chem. Chem. Phys.* 15 (2013) 14513–14824, <https://doi.org/10.1039/c3cp52154k>.
- [110] Y. Zhong, X. Wan, Z. Ding, L.L. Shaw, New dehydrogenation pathway of LiBH₄ + MgH₂ mixtures enabled by nanoscale LiBH₄, *Int. J. Hydrogen Energy* 41 (2016) 1–2.
- [111] H. Lee, J. Lee, D.Y. Kim, J. Park, Y.-T. Seo, H. Zeng, I.L. Moudrakovski, C.I. Ratcliffe, J.A. Ripmeester, Tuning clathrate hydrates for hydrogen storage, *Nature* 434 (2005) 743–746, <https://doi.org/10.1038/nature03457>.
- [112] G.A. Olah, A. Goepfert, G.K.S. Prakash, *Beyond Oil and Gas: the Methanol Economy*, dated and WILEY-VCH Verlag GmbH & Co. KGaA, Weinheim, 2009.
- [113] S. Niaz, T. Manzoor, A. Hussain, *Hydrogen Storage: Materials, Methods and Perspectives* vol. 50, (2015), pp. 457–469, <https://doi.org/10.1016/j.rser.2015.05.011>.
- [114] A.T. Raissi, *Technoeconomic Analysis of Area II Hydrogen Production - PART II Hydrogen from Ammonia and Ammonia-borane Complex for Fuel Cell Applications* vol. 3, (2002), pp. 1–17.
- [115] H. Leng, Q. Li, Improved dehydrogenation properties of Mg (BH₄)₂ · 2NH₃ combined with LiAlH₄, *Int. J. Hydrogen Energy* 40 (2015) 8362–8367, <https://doi.org/10.1016/j.ijhydene.2015.04.109>.
- [116] IEA, Key World Energy Statistics 2015, Statistics (Ber), (2015), p. 82, <https://doi.org/10.1787/9789264039537-en>.
- [117] G. Gahleitner, Hydrogen from renewable electricity: an international review of power-to-gas pilot plants for stationary applications, *Int. J. Hydrogen Energy* 38 (2012) 2039–2061, <https://doi.org/10.1016/j.ijhydene.2012.12.010>.
- [118] AMF Fuel Information System, Methanol, Technol. Collab. Program. Adv. Mot. Fuels (AMF TCP) within a Framework, Int. Energy Agency (IEA), 2016, http://iea-amf.org/content/fuel_information/methanol, Accessed date: 9 November 2016.
- [119] A. Exance, Carbon Dioxide-to-methanol Catalyst Ignites “fuel from Air” Debate, (2016).
- [120] J. Kothandaraman, A. Goepfert, M. Czaun, G.A. Olah, G.K.S. Prakash, Conversion of CO₂ from Air into Methanol Using a Polyamine and a Homogeneous Ruthenium Catalyst, (2016), pp. 2–5, <https://doi.org/10.1021/jacs.5b12354>.
- [121] UNEP, *Global Chemicals Outlook towards Sound Management of Chemicals*, (2013).
- [122] P. Stefenson, Why methanol is important to Stena, Liq. Wind Semin, 2017.
- [123] IMAREST, First Methanol-burning Oceangoing Ships Delivered, IMAREST, 2016, <http://www.imarest.org/themarineprofessional/item/2309-first-methanol-burning-oceangoing-ships-delivered>.
- [124] M. Kotisaari, Dimethyl Ether Reforming for High Temperature PEM Fuel Cells, (2009).
- [125] P.J. Bonitatibus, S. Chakraborty, M.D. Doherty, O. Siclován, W.D. Jones, G.L. Soloveichik, Reversible catalytic dehydrogenation of alcohols for energy storage, *Proc. Natl. Acad. Sci. Unit. States Am.* 112 (2015) 1687–1692, <https://doi.org/10.1073/pnas.1420199112>.
- [126] I. Hannula, *Synthetic Fuels and Light Olefins from Biomass Residues, Carbon Dioxide and Electricity. Performance and Cost Analysis*, Dissertation 107 VTT Technical Research Centre of Finland Ltd, 2015.
- [127] A. Tremel, P. Wasserscheid, M. Baldauf, T. Hammer, Techno-economic analysis for the synthesis of liquid and gaseous fuels based on hydrogen production via electrolysis, *Int. J. Hydrogen Energy* 40 (2015) 11457–11464, <https://doi.org/10.1016/j.ijhydene.2015.01.097>.
- [128] G. Thomas, G. Parks, Potential Roles of Ammonia in a Hydrogen Economy, (2006).
- [129] A. Reiter, Combustion and Emissions Characteristics of a Compression-ignition Engine Using Dual Ammonia-diesel Fuel, Paper 10560 Iowa State University, 2009.
- [130] DieselNet Technology Guide, (2016) <https://www.dieselnets.com/technical.html>.
- [131] Ammonia - Toxicological Overview, (2015).
- [132] G. Fulks, G.B. Fisher, K. Rahmoeller, M.-C. Wu, E. D’Herde, J. Tan, A review of solid materials as alternative ammonia sources for lean NO_x reduction with SCR. SAE paper 2009-01-0907, Soc. Automot. Eng., © 2009 SAE International, 2009.
- [133] A. Klerke, C.H. Christensen, J.K. Nørskov, T. Vegge, Ammonia for hydrogen storage: challenges and opportunities, *J. Mater. Chem.* 18 (2008) 2285–2392, <https://doi.org/10.1039/b720020j>.
- [134] ISO 22241-1:2006(en) Diesel engines — NO_x reduction agent AUS 32 — Part 1: Quality requirements, (2006).
- [135] AdBlue, Material Safety Data Sheet vol. 5, (2013), pp. 1–5.
- [136] K. Lehtoranta, H. Vesala, P. Koponen, S. Korhonen, Selective catalytic reduction operation with heavy fuel oil: NO_x, NH₃, and particle emissions, *Environ. Sci. Technol.* 49 (2015) 4735–4741, <https://doi.org/10.1021/es506185x>.
- [137] A. Solla, M. Westerholm, C. Söderström, K. Tormonen, T. Härmälä, T. Nissinen, J. Kukkonen, Effect of ammonium formate and mixtures of urea and ammonium formate on low temperature activity of SCR systems, SAE Paper 2005-01-1856. Soc. Automot. Eng., © SAE International, 2005, p. 8.
- [138] W.I.F. David, Effective hydrogen storage: a strategic chemistry challenge, *Faraday*

- Discuss 151 (2011) 399–414, <https://doi.org/10.1039/c1fd00105a>.
- [139] K. Kunze, O. Kircher, *Cryo-compressed Hydrogen Storage*, (2012).
- [140] T. Riis, E.F. Hagen, P.J.S. Vie, Ø Ulleberg, Hydrogen production and storage. R&D priorities and gaps, *Hydrog. Implement. Agreem.* (2006) 33, [https://doi.org/10.1016/0360-3199\(88\)90106-1](https://doi.org/10.1016/0360-3199(88)90106-1).
- [141] AdAmmin.eTM - the Solid Ammonia Material, (2016) <http://www.amminex.com/products/adammine.aspx>, Accessed date: 26 August 2016.
- [142] Y. Zhang, M. Markiewicz, J. Filser, S. Stolte, Toxicity of a Quinaldine-based Liquid Organic Hydrogen Carrier (LOHC) System toward Soil Organisms *Arthrobacter Globiformis* and *Folsomia candida* vol. 52, (2018), pp. 258–265, <https://doi.org/10.1021/acs.est.7b04434>.
- [143] Anon, IEA Advanced Motor Fuels - Fuel Information System, (n.d.). http://www.iea-amf.org/content/fuel_information/fuel_info_home.
- [144] IPHE, Hydrogen Storage, (n.d.).
- [145] W. Arlt, P. Wasserscheid, Arrangement and Method for Operating Hydrogen Filling Stations, US20160061383 A1 (2016).
- [146] Chiyoda, Hydrogen Supply from Russia to Japan by SPERA Hydrogen Technology Reliability No. 1 EPC Company, (2015).
- [147] Y. Okada, M. Shimura, Development of large-scale H₂ storage and transportation technology with Liquid Organic Hydrogen Carrier (LOHC), *Tech. Pap. Jt. GCC-JAPAN Environ. Symp. Febr.* 2013, p. 2013.
- [148] Chiyoda's Hydrogen Supply Business, (n.d.). <https://www.chiyodacorp.com/en/service/spera-hydrogen/>.
- [149] E. Newson, T.H. Haueter, P. Hottinger, von F. Roth, G.W.H. Scherer, T.H.H. Schucan, Seasonal storage of hydrogen in stationary systems with liquid organic hydrides, *Int. J. Hydrogen Energy* 23 (1998) 905–909.
- [150] M. Aziz, Integrated hydrogen production and power generation from microalgae, *Int. J. Hydrogen Energy* 41 (2015) 104–112, <https://doi.org/10.1016/j.ijhydene.2015.10.115>.
- [151] C. Krieger, K. Müller, W. Arlt, Coupling of a liquid organic hydrogen Carrier system with industrial heat, *Chem. Eng. Technol.* 39 (2016) 1570–1574, <https://doi.org/10.1002/ceat.201600180>.
- [152] C. Krieger, K. Müller, W. Arlt, Thermodynamic analysis of reversible hydrogenation for heat storage in concentrated solar power plants, *Sol. Energy* 123 (2016) 40–50, <https://doi.org/10.1016/j.solener.2015.11.007>.
- [153] G.W.H. Scherer, E. Newson, Analysis of the seasonal energy storage of hydrogen in liquid organic hydrides, *Int. J. Hydrogen Energy* 23 (1998) 19–25.
- [154] S. Dürr, M. Müller, H. Jorschick, M. Helmin, A. Bösmann, R. Palkovits, P. Wasserscheid, Carbon dioxide-free hydrogen production with integrated hydrogen separation and storage, *ChemPubSoc Eur.* 10 (2017) 42–47, <https://doi.org/10.1002/cssc.201600435>.
- [155] A. Sekanina, E. Pucher, H₂-Automotive: New Vehicle Technologies and Propulsion Systems, F2006SC01 (2006).
- [156] T.D. Elmoe, R.Z. Sørensen, U. Quaade, C.H. Christensen, J.K. Norskov, T. Johannessen, A high-density ammonia storage/delivery system based on Mg (NH₃)₆Cl₂ for SCR – DeNO_x in vehicles, *Chem. Eng. Sci.* 61 (2006) 2618–2625, <https://doi.org/10.1016/j.ces.2005.11.038>.
- [157] K. Müller, J. Geng, W. Arlt, Reversible vs. Irreversible conversion of Hydrogen : how to store energy efficiently? *Energy Technol.* 1 (2013) 42–47, <https://doi.org/10.1002/ente.201200022>.
- [158] M. Eypasch, M. Schimpe, A. Kanwar, T. Hartmann, S. Herzog, T. Frank, T. Hamacher, Model-based techno-economic evaluation of an electricity storage system based on Liquid Organic Hydrogen Carriers, *Appl. Energy* 185 (2017) 320–330, <https://doi.org/10.1016/j.apenergy.2016.10.068>.
- [159] A.U. Pradhan, A. Shukla, J. V Pande, S. Karmarkar, R.B. Biniwale, A feasibility analysis of hydrogen delivery system using liquid organic hydrides, *Int. J. Hydrogen Energy* 36 (2010) 680–688, <https://doi.org/10.1016/j.ijhydene.2010.09.054>.
- [160] C. Yang, J. Ogden, Determining the lowest-cost hydrogen delivery mode, *Int. J. Hydrogen Energy* 32 (2007) 268–286, <https://doi.org/10.1016/j.ijhydene.2006.05.009>.
- [161] K. Reddi, A. Elgowainy, N. Rustagi, E. Gupta, Techno-economic analysis of conventional and advanced high-pressure tube trailer configurations for compressed hydrogen gas transportation and refueling, *Int. J. Hydrogen Energy* (2018) 1–11, <https://doi.org/10.1016/j.ijhydene.2018.01.049>.
- [162] P. Cazzola, G. Morrison, H. Kaneko, F. Cuenot, A. Ghandi, L. Fulton, Production Costs of Alternative Transportation Fuels, (2013).
- [163] R. McGill, W. Remley, K. Winther, Alternative Fuels for Marine Applications (AMF Annex 41), (2013), p. 108 http://iea-amf.org/app/webroot/files/file/AnnexReports/AMF_Annex_41.pdf.
- [164] G.B. Haxel, J.B. Hedrick, G.J.E. Orris, Rare Earth Elements — Critical Resources for High Technology, (2002) <http://geopubs.wr.usgs.gov/fact-sheet/fs087-02/>.
- [165] P. Argust, Distribution of boron in the environment, *Biol. Trace Elem. Res.* 66 (1998) 131–143.
- [166] Anon, Heat Transfer Fluids Market Analysis By Product (Silicones & Aromatics, Mineral Oils, Glycol), By Application (Oil & Gas, Chemical Industry, Concentrated Solar Power (CSP), Food & Beverages, Plastics, Pharmaceuticals, HVAC) And Segment Forecasts To 2022, (n.d.). <http://www.grandviewresearch.com/industry-analysis/heat-transfer-fluids-market>.
- [167] Anon, Carbazole (see also EP-A-410214, EP 2470503 B1), (n.d.). www.chemicaland21.com/specialtychem/finechem/CARBAZOLE.htm.
- [168] R.K. Ahluwalia, T.Q. Hua, J.-K. Peng, Technical Assessment of Organic Liquid Carrier Hydrogen Storage Systems for Automotive Applications, (2011).
- [169] Mineral commodity Summaries, (2013).
- [170] Anon, Platinum-Group Metals: World Production, By Country, (n.d.). http://www.indexmundi.com/en/commodities/minerals/platinum-group_metals/platinum-group_metals_t5.html.
- [171] O.M. Yaghi, Hydrogen Storage in Metal-organic Frameworks, (2011).
- [172] US DOE, Targets for Onboard Hydrogen Storage Systems for Light-duty Vehicles, (2009).
- [173] D. Saha, Z. Wei, S. Deng, Equilibrium, kinetics and enthalpy of hydrogen adsorption in MOF-177, *Int. J. Hydrogen Energy* 33 (2008) 7479–7488, <https://doi.org/10.1016/j.ijhydene.2008.09.053>.
- [174] A. Karmakar, C. Aardah, T. Autrey, Recent developments on hydrogen release from ammonia borane dehydrogenation, *Mater. Matters* 2 (2007).